Ultrabright light emission properties of all-inorganic and hybrid organic-inorganic copper(I) halides

Dhritiman Banerjee[†], *Bayram Saparov*[†*]

†D*epartment of Chemistry and Biochemistry, University of Oklahoma, 101 Stephenson Parkway, Norman, Oklahoma 73019, United States*

[*]*Author to whom correspondence should be addressed: saparov@ou.edu*

Abstract

All-inorganic and hybrid copper(I) halides have recently emerged as candidate optical materials due to their extremely high light emission efficiencies, non-toxic and earth-abundant elemental compositions, and low-cost solution processibility. Originally inspired and motivated by the research on the halide perovskites family, the development of copper(I) halide light emitters has been following its unique path. In this perspective, we discuss the distinct low-dimensional crystal structures of all-inorganic halides, which enable strong charge localization and formation of room-temperature self-trapped excitonic (STE) states, giving rise to largely Stoke-shifted light emission with near-unity quantum yields. Due to their unique electronic structures, all-inorganic copper halides are predominantly blue emitters with unusually weak tunability of their optical properties (e.g., halide substitution has a minimal impact on their photoluminescence properties). These shortcomings paved the way for the exploration of more robust and diverse families of hybrid organic-inorganic copper(I) halides, which are discussed next. Our discussions of crystal and electronic structures and optical properties of all-inorganic and hybrid Cu(I) halides are complemented by the reported uses of these materials in optoelectronic applications. Finally, we identify remaining fundamental questions, knowledge gaps and practical challenges and outline several paths forward for addressing these issues, including through new materials discovery and in-depth studies of photophysics of Cu(I) halides and derivative materials.

1. Introduction

In the past decade, metal halide perovskites have attracted great attention, especially lead halide perovskites, due to their outstanding performance in optoelectronic devices such as solar cells and LEDs.[1,2] Lead halide perovskites possess many advantageous attributes for light emission applications including tunable band gaps and photoluminescence emission colors, high photoluminescence quantum yields (PLQYs) and long exciton diffusion pathways, to name just a few.[3] The most prominent family among the light-emitting lead halide perovskites is $CsPbX_3$ (X= Cl, Br, I), which has been extensively investigated in the past for next-generation optoelectronics.[4] Despite the outstanding optoelectronic properties of lead halide perovskites, lead toxicity and instability of some members under ambient air, irradiation, and heat exposure are sources of concern.[5] These major concerns continue to motivate the search for the next generation of alternative metal halides that are simultaneously both free of Pb, earth-abundant, stable and environmentally friendly, and also can achieve parity in the optoelectronic properties and performance displayed by lead halide perovskites. In the past decade, great many metal cations have been studied as potential alternatives for Pb(II) including Cu(I), Ag(I), Sn(II), Mn(II), Sb(III), Bi(III), In(III) and Sn(IV).[1,6] Due to the differences in oxidation states, sizes and coordination environment preferences of metals, not all of these substitutions result in compounds with perovskite structure type. Nevertheless, this research has yielded many new compounds with unique crystal and electronic structures, and promising optical and electronic properties; in fact, some of these novel metal halides display optical and electronic properties that can not only rival that of lead halide perovskites, but also outperform them. Among these, Cu(I)-based halides with non-perovskite structures have emerged in the past 5 years as some of the highest efficiency light emitters that combine earth-abundant, nontoxic and low-cost elemental compositions, and accessibility via both low-temperature solution processing and high-temperature synthesis.[7,8]

Interest in preparation and characterization of copper halide perovskites predate the recent interest in halide perovskites as photovoltaic (PV) materials.[9] Just like for other transition metal halide perovskites, early studies focused on the intriguing magnetic properties of layered Cu(II) halides.[10] These Cu(II) halides belong to a subgroup of a large family of low-dimensional metal halide perovskites derived from the parent 3D ABX_3, where A is an organic or inorganic cation of suitable size, B is typically a divalent metal cation, and X is a halide ion. In the case of Cu(II) halides, the inorganic layers display unique distortion (*aka* antiferrodistortive arrangement) due to the presence of strongly Jahn-Teller active Cu^{2+} ($3d^9$) in octahedral coordination environment. Most recently, after the emergence of $MAPbI_3$ as a high performance semiconductor, 2D layered Cu(II) halide perovskites have been revisited as potential Pb-free semiconductors for optoelectronic applications.[9] Note here that in addition to the structural distortions, the presence of unfilled *d*-states leads to a significantly different band structures of Cu(II) halides as compared *p*-block metal (e.g., Pb(II), Sb(III), In(III) etc.) halide perovskites.[9] In contrast, Cu(I) with $3d^{10}$ electronic configuration is valence isoelectronic with *p*-block metal cations such as Ga(III), In(III) and Tl(III), and therefore, could be a better candidate (from the electronic perspective) for the B cation role. However, in comparison to the studies on Cu(II) halides, little work had been done on optoelectronic characterization and applications prospects of all-inorganic and hybrid organic-inorganic Cu(I) halides until recent years. This is because the inclusion of Cu(I) into halide perovskite structure requires additional compositional and structural changes to account for the monovalent charge state of copper (as opposed to Pb^{II} in $APbX_3$ halide perovskites).

One possible avenue for such heterovalent substitutions in halide perovskites is exemplified by the large family of $A_2B^IB^{III}X_6$ double perovskites (*aka* elpasolites) in which divalent lead is replaced by a pair of a monovalent (e.g., Ag(I), Tl(I)) and trivalent (e.g., Sb(III), Bi(III), In(III)) metal cations. [11, 12] In early 2017, our group started working on preparation of substitution analogs of double perovskites containing group 11 (Ag and Cu) and rare-earth metal cations such as Cs_2AgCeX_6 and Cs_2CuCeX_6. Among these, $Cs_2AgCeCl_6$ is a known compound with the reported preparation involving solvothermal synthesis.[13] Our follow-up synthetic work led to the isolation and serendipitous discovery of excellent optical properties of $Cs_3Cu_2X_5$.[14] While Cu(I) containing double perovskites could not be prepared, these early experiments formed the basis of our many years research work in the field of photoluminescent (PL) Cu(I) halides. All Cu(I)-based halides reported so far exhibit low-dimensional crystal structures, and these structures feature non-octahedral building blocks (most typically, tetrahedral Cu^IX_4 units), yet their light emission properties comfortably rival (or surpass) that of lead halide perovskites. Therefore, the major takeaway from this research is that *beyond perovskites, non-perovskite metal halides also exhibit remarkable photophysical properties that can be utilized in practical applications.*

An exciting development in this field is a growing number of studies on nanomaterials based on Cu(I) halides, which will not be covered in this work. Similarly, Cu(I) halides featuring direct Cu-organic bonding (i.e., organometallic Cu(I) halides) have also been of interest in the past several decades, however, since their crystal and electronic structures are markedly different from that of all-inorganic and hybrid organic-inorganic Cu(I) halides, these are also not included in this literature review. In this focused perspective, we summarize synthesis, structural and optoelectronic properties, and potential applications of bulk Cu(I) halides with a major focus on the developments in the field in recent years. This work is concluded with discussions of unanswered questions and exciting future research directions from our perspective.

2. All-inorganic copper halides

I. Syntheses and crystal structures of $CsCu_2X_3$, A_2CuX_3, $A_3Cu_2X_5$, and mixed anion Cu(I) halides

Progressive reduction in crystal structure dimensionality from the parent 3D $APbX_3$ lead halide perovskites down to 0D lead halides is known to lead to increasing charge localization on the inorganic anionic structural framework, which in turn results in increasing exciton binding energies, presence of

room temperature stable excitons and intense excitonic emission at or near room temperature.[15] All-inorganic copper(I) halides form either as 1D or 0D structures that can be classified into four different families (Figure 1): the $CsCu_2X_3$ ("123") family with the $CsCu_2Cl_3$ type structure (space group *Cmcm*, Pearson's symbol *oS*24), the A_2CuX_3 ("213") family with the K_2CuCl_3 type structure (s.g. *Pnma*, P.s. *oP*24), the $A_3Cu_2X_5$ ("325") family with the $Cs_3Cu_2Cl_5$ (s.g. *Cmcm*, P.s. *oS*48) and $Cs_3Cu_2I_5$ (s.g. *Pnma*, P.s. *oP*40) structure types, and $Cs_5Cu_3Cl_6I_2$ ("mixed anions family"). Here, the discussion will be limited to all-inorganic members of these families, i.e., the *A* site cation is limited to Cs, Rb, and K, which have been extensively studied in literature. However, a survey of Pearson's structural database[16] suggests that other poorly studied known members of these families exist, e.g., where the *A* site is occupied by NH_4^+ such as in the case of $(NH_4)_2CuX_3$.[17] Furthermore, continued synthetic and characterization efforts are likely to result in a significant expansion of these to include a variety of hitherto unknown members of these structural families featuring organic cations on the *A* site.

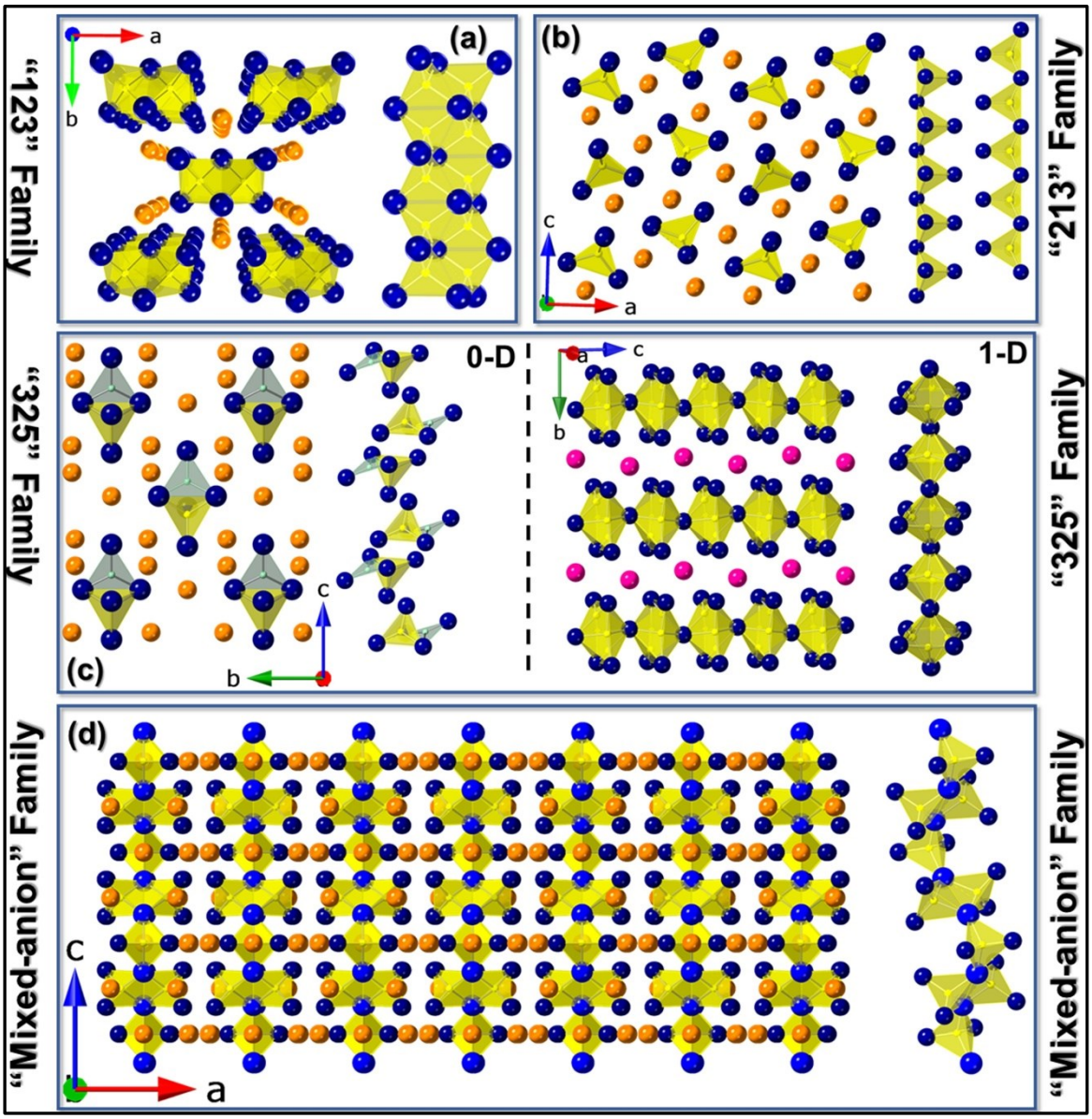

Figure 1. Polyhedral representations of the crystal structures of different families of alkali copper halides. (a) One-dimensional (1D) crystal structure of $CsCu_2X_3$ (X = Cl, Br, I) features $^1_\infty[Cu_2X_3]^-$ anionic double chains made of edge-sharing tetrahedra (on the right) extending along the *c*-axis. The orange, yellow, and dark blue spheres represent Cs, Cu, and *X*, respectively. (b) One-dimensional (1D) crystal structure of A_2CuX_3 (A = K, Rb; X = Cl, Br) features $^1_\infty[CuX_3]^{2-}$ anionic chains made of corner-sharing tetrahedra (on the right) extending along the *b*-axis. The orange, yellow, and dark blue spheres represent *A,* Cu, and *X*, respectively. (c) (left) Zero-dimensional

(0D) crystal structure of $Cs_3Cu_2X_5$ (X = Cl, Br, I) contains ${}^{0}_{\infty}[Cu_2X_5]^{3-}$ dimers separated by Cs^+ cations. (right) The second polymorph of $Cs_3Cu_2Cl_5$ exhibits 1D structure containing complex tetrameric cluster units that extend along the chain propagation direction via corner-sharing. The orange, yellow, pastel green and dark blue spheres represent Cs, two sites of Cu, and X, respectively. The $[Cu_2X_5]^{3-}$dimers are made of trigonal planar CuX_3 units sharing common edges with tetrahedral CuX_4 units. (d) $Cs_5Cu_3Cl_6I_2$ features 1D zigzag ${}^{1}_{\infty}[Cu_3Cl_6I_2]^{5-}$ chains. The orange, yellow, dark blue and blue spheres represent Cs, Cu, Cl, and I, respectively.

(a) The 123 family

One of the key advantages of all-inorganic Cu(I) halides is the fact that they can be prepared using both wet chemistry and solid-state synthesis techniques. In a recent study by Roccanova et al., members of the "123" family were prepared using solid-state synthesis and their photophysical properties were characterized.[18] In fact, these compounds may also be melt-processable as the TGA/DSC studies suggest congruent melting at 270, 351, and 374 °C for $CsCu_2Cl_3$, $CsCu_2Br_3$, and $CsCu_2I_3$, respectively. In a follow-up study, Lin et al. synthesised $CsCu_2I_3$ as colorless, rod-shaped single crystals using the antisolvent infiltration method.[19] The accessibility of the compounds in this family through a variety of synthesis techniques is a major advantage for their potential practical applications.

The recent works confirmed the results of earlier studies reporting that $CsCu_2Cl_3$, $CsCu_2Br_3$ and $CsCu_2I_3$ are isostructural and adopt the $CsCu_2Cl_3$ type structure in the orthorhombic space group *Cmcm*. This 1D structure features ${}^{1}_{\infty}[Cu_2X_3]^{-}$ anionic double chains extending along the *c*-axis. The basic building block of these chains are Cu^IX_4 tetrahedra that share common edges to form a ribbon-like structure (Figure 1(a)). Interestingly, the smallest separation between the $[Cu_2X_3]^{-}$ chains as measured by interchain X–X distance is slightly less than the sum of halide radii (i.e., $d(X–X) < 2r_X$ can be found in $CsCu_2X_3$) suggesting close-packing of the halide sublattice and orbital interactions between the adjacent copper(I) halide chains. This could explain the fact that among all-inorganic Cu(I) halides, $CsCu_2X_3$ demonstrate the lowest light emission efficiencies (see below). Therefore, further work aimed at preparation of ACu_2X_3 with increased inter-chain distances and greater charge localization (e.g., via incorporation of larger organic cations) is warranted to improve light emission efficiencies of materials in this family.

Since $CsCu_2X_3$ are isostructural, alloying on the halide site to obtain solid solutions could be possible in this family. This is supported by the reported preparation of $CsCu_2Cl_{1.5}Br_{1.5}$ and $CsCu_2Br_{1.5}I_{1.5}$. Following Vegard's law, the reported crystallographic parameters in this family increase linearly with the increase in the halide size.[18] The increased disorder on the halide site, however, negatively impacts light emission properties as these alloyed compositions exhibit quenched PL with minimal efficiencies (<1%). While the detrimental impact of halide alloying can be attributed to the increased defect and impurity concentration, at the atomic level, the impact of non-uniform coordination environments around individual copper(I) atoms cannot be dismissed. The importance of local coordination environment of Cu has been demonstrated by a recent work reporting pressure-dependent structural and optical properties of $CsCu_2I_3$. This compound displays pressure-induced phase change due to inter- and intra-tetrahedral distortions under compression, which significantly enhance its yellow light emission properties (slight shifts in the PL peak positions occur).[20] In-depth computational studies showed that three distinct self-trapped excitonic (STE) states corresponding to different excited state structural distortions can be stabilized in the "123" family.[21] The relative stabilities of these STE states are halogen-dependent, which has been broadly explained as arising from the different degrees of bond ionicity and halide size trends in $CsCu_2Cl_3$, $CsCu_2Br_3$, and $CsCu_2I_3$. In $CsCu_2X_3$ (X = Br, I), the emissive STE state corresponds to the lowest energy STEs whereas the metastable STE is the emissive state in $CsCu_2Cl_3$. These results suggest that atomic level tuning of bond distances and packing of polyanionic units in Cu(I) halides is necessary for obtaining optimized and controllable photoemission.

(b) The 213 family

The direct replacement of Cs with lighter alkali metals such as Rb and K in $CsCu_2X_3$ is not possible. Such attempts result in A_2CuX_3 (A = K, Rb; X = Cl, Br) compounds belonging to the "213" family of copper(I) halides. Two groups independently reported preparation, crystal and electronic structures, and outstanding optical properties of Rb_2CuX_3 in 2019. Yang et al. synthesized 200 mm rod-shaped single crystals of Rb_2CuBr_3 via the low-temperature crystallization method.[22] Creason et al. showed that Rb_2CuCl_3 and Rb_2CuBr_3 can be obtained using both solid-state methods and slow cooling of saturated solutions to obtain polycrystalline powders and single crystals, respectively.[23] Further synthesis work showed that compounds in the "213" family such as K_2CuX_3 can also be obtained by using molten salt as flux, liquid-liquid and vapor-liquid diffusion growth of single crystals.[7] Such ease of preparation is one of the major advantageous aspects of all-inorganic Cu(I) halides, e.g., as compared to many hybrid organic-inorganic metal halides that cannot be prepared via high-temperature and/or vacuum processing methods.

A_2CuX_3 crystallize in the orthorhombic space group *Pnma* with a 1D crystal structure made up of $^1_\infty[CuX_3]^{2-}$ chains separated by A^+ cations.[23] Unlike the $^1_\infty[Cu_2X_3]^-$ anionic double chains in the "123" family, $^1_\infty[CuX_3]^{2-}$ are single chains formed by corner-sharing Cu^IX_4 tetrahedra extending along the *b*-axis (Figure 1(b)). Despite the fact that both the "123" and "213" families are 1D in terms of the connectivity of Cu-X network, a higher degree of charge localization is expected in the case of the "213" family. This because interchain distances are greater in the "213" family as measured by the closest halide-halide distances in neighbouring $^1_\infty[CuX_3]^{2-}$ chains. Thus, the shortest interchain distance in K_2CuCl_3 is d(Cl–Cl) = 3.669 Å, slightly higher than twice of the chloride anion radius. Furthermore, this interchain distance is tunable through alkali metal substitutions – the interchain distances of d(Cl–Cl) = 3.864 Å is expectedly longer in Rb_2CuCl_3. In addition to the longer interchain distances, the distances between Cu centers are also longer within the $[CuX_3]^{2-}$ chains of A_2CuX_3 due to the different connectivity mode in these two families (corner- vs edge-sharing). As stated above, these intricate details are likely to be very important in the observed contrasting photophysical properties of these two families, members of the "213" family exhibit near-unity PLQY blue light emission with unusually weak PL tunability through alkali metal and halide substitutions (see section II). The discussed differences in crystal structures may also explain the observed differences in valence band (VB) dispersions for the "123" and "213" families. As representative examples, a comparison of the reported band structures of $CsCu_2Cl_3$ and K_2CuCl_3 suggests that while VB is dominated by Cu-3*d* states in both cases, $CsCu_2Cl_3$ has much more dispersive VB that extends from 0 to -2 eV vs 0 to -1 eV for K_2CuCl_3.[18,7] In fact, the greatest valence band dispersion in the "123" family is observed in $CsCu_2I_3$ because of the larger size of I^- anion, which allows orbital interactions with the neighboring chains, giving rise to three-dimensionally mobile holes. [24, 25] While some inferences can be made through such indirect structural comparisons, it should be noted here that more work is needed to clearly pinpoint the impact of each structural parameter on the observed physical property differences in Cu(I) halides.

Yet another important materials property, stability of materials, can also be tied to their crystal structures. $CsCu_2X_3$ with tightly packed structures are reported to be stable in air (for months), and show excellent thermal stability (up to 495 °C).[18] In contrast, while Rb_2CuX_3 with distinctly larger interchain distances are also thermally stable (no significant weight loss up to 475 °C), they are unstable in air. For example, Rb_2CuCl_3 degrades within a day in moist air forming RbCl and $Rb_2CuCl_4{\cdot}2H_2O$. K_2CuX_3 can be viewed as the chemically pressurised derivatives of Rb_2CuX_3 with shorter interchain distances,[7] and they demonstrate greatly improved air-stability as compared to Rb_2CuX_3. As is clear from these discussions, more compositional and structural tuning can and should be done in these families to increase charge localization, increase excitonic binding energies and emission efficiencies, and improve

materials stability. For the latter, since the mechanism of degradation involves oxidation of Cu(I) to Cu(II), a direct replacement of copper with silver can be considered. This has been demonstrated by the preparation and characterization of the Ag analogues of the "213" copper halides, A_2AgX_3 (A = Rb, Cs, NH_4; X = Cl, Br, I).[26,27] Note that not all of A_2AgX_3 are isostructural to A_2CuX_3; while Cs_2AgX_3 adopt the K_2CuCl_3 type structure and are isostructural to A_2CuX_3, the use of smaller A^+ cations in Rb_2AgX_3, $(NH_4)_2AgX_3$ and K_2AgX_3 leads to the K_2AgI_3 type structure (Figure 2).[26] Both structure types are largely similar and feature $^1_\infty[AgX_3]^{2-}$ chains separated by the A^+ cations. However, they differ in terms of relative packing of $^1_\infty[AgX_3]^{2-}$ anionic chains and A^+ cations. The impact of this different packing is seemingly negligible as both structure types are in the orthorhombic space group *Pnma*, i.e., the different packing does not lead to a symmetry change. In addition, the interchain distances remain largely unchanged, e.g., the interchain distances in Rb_2AgBr_3 and Rb_2CuBr_3 with the K_2AgI_3 and K_2CuCl_3 type structures, respectively, are nearly identical (~4.09 Å). Importantly, confirming the intended materials design idea, Rb_2AgX_3 demonstrate much improved air stability as compared to the poor stability displayed by Rb_2CuX_3. The success in materials stability improvement achieved by the replacement of Cu with Ag is remarkable, luminescent inks based on A_2AgX_3 can be made into patterns that are stable in water, under heat, and ultrasonication. Nevertheless, more work is needed to correlate the apparent differences in chemistries and crystal structures to the observed properties of A_2CuX_3 and A_2AgX_3; A_2CuX_3 are blue emitters with PLQYs up to 100%, whereas Ag(I) halides demonstrate broadband white light emission with much lower efficiencies (see section II).[28, 26]

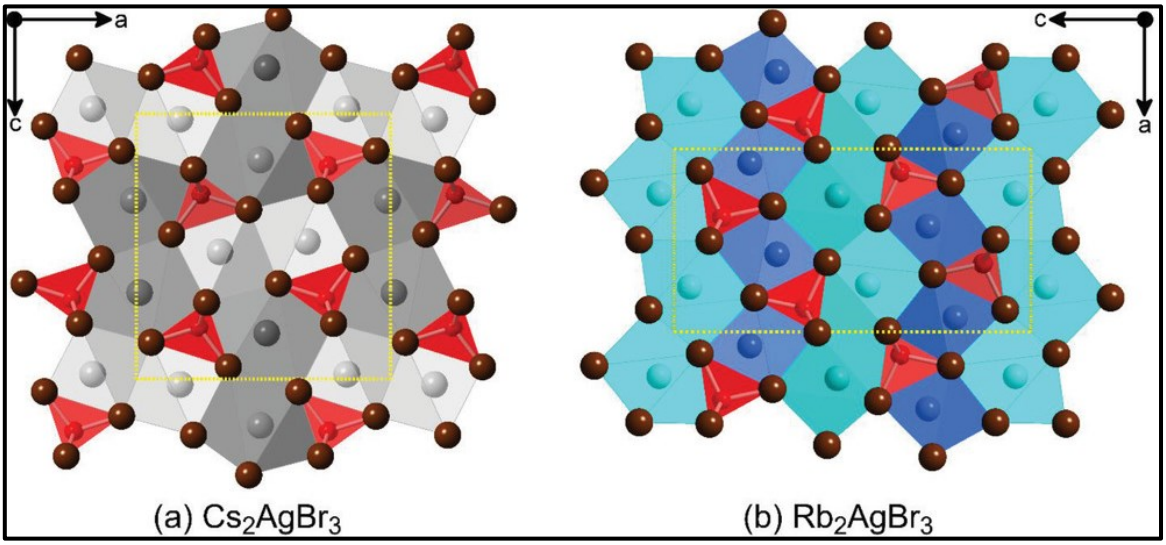

Figure 2. (a) Cs_2AgBr_3 and (b) Rb_2AgBr_3 crystallize in the K_2CuCl_3 and K_2AgI_3 type structures, respectively, featuring 1D $^1_\infty[AgX_3]^{2-}$ chains (shown in red) separated by A^+ cations. The two structure types differ only in terms of the packing of the $^1_\infty[AgX_3]^{2-}$ chains and A^+ cations, which is emphasized by showing (a) Cs1 and Cs2 in dark gray and light gray in Cs_2AgBr_3 and (b) Rb1 and Rb2 in dark blue and light blue in Rb_2AgBr_3; Ag and Br are shown in red and brown, respectively. Reprinted with permission from ref 26. Copyright 2021 John Wiley and Sons.

(c) *The 325 family*

$Cs_3Cu_2X_5$ (X = Cl, Br, I) belong to the most studied "325" family of copper halides because $Cs_3Cu_2I_5$ was the first reported high-efficiency all-inorganic Cu(I) halide light emitter in 2018.[29] Independently, our group had also been working on the "325" family of compounds after our serendipitous discovery of their outstanding optical properties while trying to obtain and characterize Cs_2CuCeX_6 double perovskites.[14] In the earlier work by Jun et al., $Cs_3Cu_2I_5$ single crystals were prepared using an

antisolvent method.[29] The solution processability of $Cs_3Cu_2I_5$ allowed deposition of this material as thin films using spin coating.[29] Other reported solution synthesis $Cs_3Cu_2I_5$ crystals include solvent evaporation crystallization at room temperature, and melt growth via vertical Bridgman method.[30] Our own work showed that $Cs_3Cu_2Br_{5-x}I_x$ ($0 \leq x \leq 5$) solid solution can be prepared by reacting stoichiometric amounts of CsX and CuX at 400 ºC.[14] Notably, solid-state synthesis produces higher purity products, especially when targeting mixed halide compositions. Since both end members, $Cs_3Cu_2Br_5$ and $Cs_3Cu_2I_5$, are isostructural and adopt the $Cs_3Cu_2I_5$ structure type, a full solid solution can be obtained with the unit cell parameters for mixed halide compositions following Vegard's law.[14] Accessibility via both wet chemistry and solid-state methods for both $CsCu_2X_3$ and $Cs_3Cu_2X_5$ provides a unique opportunity for reversible transformation between the two compounds via a solvent-assisted grinding process and solid-state methods.[31,32] Such transformations have been primarily investigated for the iodide members since $CsCu_2I_3$ and $Cs_3Cu_2I_5$ are yellow and blue emitters, respectively, and optimized mixture of the two can provide yields white-light-emitting films.[25]

$Cs_3Cu_2X_5$ (X = Cl, Br, I) crystallize in the orthorhombic *Pnma* space group adopting the $Cs_3Cu_2I_5$ structure type. Their 0D crystal structures feature $[Cu_2X_5]^{3-}$ dimeric polyanions separated by Cs^+ cations. Each $[Cu_2X_5]^{3-}$ dimer consists of a $[CuX_4]^{3-}$ tetrahedral unit attached to a trigonal planar $[CuX_3]^{2-}$ unit via edge-sharing (Figure 1(c)).[33] Notably, $Cs_3Cu_2Cl_5$ has another polymorph that crystallizes in the *Cmcm* space group featuring a 1D chain structure containing complex tetrameric cluster units (Figure. 1(c)) that extend along the chain propagation direction via corner-sharing.[34 35] The $[Cu_4Cl_6]^{2-}$ tetramers are made of two $[CuCl_3]^{2-}$ trigonal planar and two $[CuCl_4]^{3-}$ tetrahedral units sharing common edges. Interestingly, the tetramers can also be envisioned as two distorted $[Cu_2Cl_5]^{3-}$ dimers seen in the 0D polymorph fused together. The original structural reports in the Pearson's database suggest that the $Cs_3Cu_2I_5$-type $Cs_3Cu_2Cl_5$ (0D) can be obtained by a solid-state reaction of binary halides at 270 ºC for 5 days, whereas the 1D polymorph (own type) is obtained by slow cooling a water solution containing binary reactants from 70 ºC to room temperature.[36, 34, 16] We must stress here that there is a considerable amount of confusion regarding syntheses, structural and optical properties of these two polymorphs of $Cs_3Cu_2Cl_5$, requiring further work for clarification. Thus, several recent studies on $Cs_3Cu_2Cl_5$ focusing on its bright green light emission proceeded with an assumption that the compound will form in the *Pnma* space group isostructural to the other members of the $Cs_3Cu_2X_5$ family.[37, 38,39] However, the starkly contrasting green emission from $Cs_3Cu_2Cl_5$ as compared to the intense blue emission from $Cs_3Cu_2Br_5$ and $Cs_3Cu_2I_5$ within the same structure type has not been explained satisfactorily (notice that the chloride is said to give a lower energy emission as compared to higher energy emission from the bromide and iodide). An alternative scenario that the green emitting $Cs_3Cu_2Cl_5$ is the 1D polymorph crystallizing in the *Cmcm* space group with its own structure type has not been considered carefully, although there are recent reports supporting this claim.[38, 40, 41] We note that the recent publications on $Cs_3Cu_2Cl_5$ so far are contradictory in this regard as a number of studies inaccurately describe the *Cmcm* structure as made of dimers, and conversely, the *Pnma* structure as made of 1D chains.[36, 34] Altogether, a confusing picture emerges for $Cs_3Cu_2Cl_5$ in which structure types are assigned seemingly arbitrarily, and the subsequent structure description within the same publication does not agree with the assigned structure. Given the fact that $Cs_3Cu_2Cl_5$ is a superb green emitter with the reported PLQY values up 100%, fundamental investigations aimed at understanding structure-property relationships of the two polymorphs of $Cs_3Cu_2Cl_5$ are urgently needed.

(d) ***Mixed anion family***

For the isostructural Cu(I) halide families, halide alloying has been successfully achieved to obtain solid solutions for a careful analysis of structure and property trends.[14] Such anion mixing experiments involved the closest pair of halides such as in the cases of $Cs_3Cu_2Br_{5-x}I_x$ and $CsCu_2Cl_{3-x}Br_x$.[14,18] The use of chloride for alloying into an iodide compound is unlikely to work due to a large size and electronegativity differences between the two. Instead, in case both halides feature in the final product, they are likely to show strong crystallographic site preferences. In fact, this can be used to obtain new

all-inorganic Cu(I) halides with novel structure types. This strategy has been successfully applied by Hosono et al., who reported a new mixed-halide compound $Cs_5Cu_3Cl_6I_2$ (Figure 1 (d)) prepared using stoichiometric reactions of binary salts via both solid-state and solution synthesis methods.[29] From synthesis and structure perspectives, this is a major result since seemingly all known phases in the ternary A – Cu – X systems have already been prepared and characterized in recent years. Therefore, the recent report of $Cs_5Cu_3Cl_6I_2$ suggests that more compound discovery and characterization work can be done through the mixed anion approach.

The successful preparation of a new mixed-halide Cu(I) halide can not only expand the number of new compounds discovered in these families but could also provide a new design parameter; the site preferences of differing halide anions and relative energies of *p*-orbitals of I^- and Cl^- anions are likely to have an impact on the observed photophysical properties of mixed halide compounds. In the case of $Cs_5Cu_3Cl_6I_2$, its 1D crystal structure in the orthorhombic space group *Cmcm* features polyanionic $^1_\infty[Cu_3Cl_6I_2]^{5-}$ zigzag chains separated by Cs^+ cations. The individual $[Cu_3Cl_6I_2]^{5-}$ chain consists of tetrahedral $[CuCl_2I_2]$ building blocks that are connected to each other via corner- and edge-sharing connections. The preferred distribution of anions is such that only the I^- ions serve as the bridge halides both in corner- and edge-sharing connections. The fact that the analogous compound $Cs_5Cu_3Cl_6Br_2$ could not be prepared[24] suggests that strong halide site preference is necessary to stabilize this structure. In the original study reporting $Cs_5Cu_3Cl_6I_2$, the authors observed that PL peak of this compound lines in between that of $Cs_3Cu_2I_5$ and $Cs_3Cu_2Cl_5$, however, since the midgap emission in these compounds are attributed to STEs and observed optical properties do not follow the rigid band shift model, this observation seems purely coincidental.[24] Instead, the work on mixed halide anions shows that the structural differences between $Cs_5Cu_3Cl_6I_2$ and $Cs_3Cu_2X_5$ is responsible for the observed optical property differences. In fact, the authors speculated that the I-Cl^- dimer V_K centers form in $Cs_5Cu_3Cl_6I_2$ that promote hole localization, which in turn lead to the formation of stable STE states. [24] Therefore, the halogen makeup of the materials is important as they play an important role in the proposed hole trapping and STE formation mechanism.

II. Optical Properties

All-inorganic Cu(I) halides are typically STE-based blue emitters with very high emission efficiencies up to 100% at room temperature. Their record high emission efficiencies allow their consideration for a number of practical applications such as solid-state lighting, temperature and radiation sensing and anti-counterfeiting. This chapter summarizes the unique photophysical properties of each all-inorganic Cu(I) halide family and the literature-reported practical applications thereof.

(a) The 123 family

$CsCu_2X_3$ display tunability of PL emission through halogen substitution (X= Cl, Br, I), which is in stark contrast to the other blue emitting all-inorganic Cu(I) halide families that are unusually insensitive to halide substitution.[14] Roccanova et al. demonstrated that light emission from $CsCu_2X_3$ redshifts from green (527 nm) in $CsCu_2Cl_3$ to yellow (576 nm) in $CsCu_2I_3$ (Figure 3 (a)-(b)).[14] The details of the photoluminescence properties of $CsCu_2X_3$ have been summarised below in Table 1. While this ~50 nm change in the PL peak position is visible to a naked eye and is much greater than that reported for the other all-inorganic Cu(I) halide families, the PL peak shifts reported for $CsPbX_3$ are much higher.[4] This is because the latter demonstrate (near) band-to-band emission whereas $CsCu_2X_3$ emit from midgap STE states, leading to very large 208-242 nm Stokes shifts and very broad PL emission peaks with full width at half maximum (FWHM) values of 102-126 nm. Within the 123 family, emission efficiency decreases from PLQY of 48% for $CsCu_2Cl_3$ Cl to PLQY of only 3.23% in $CsCu_2I_3$. In octahedral metal halide structures including halide perovskites, the observed optical property trends including PLQYs are often tied to the degree of octahedral distortion – correlations have been made between the increase in the octahedral distortion with the increase in Stokes shifts, FWHMs, and PLQYs.[42,43,44,45] Analogous

studies on the effect of tetrahedral distortion on optoelectronic properties of metal halides have rarely been reported. For the $CsCu_2X_3$ family, Roccanova et al. report decreasing tetrahedral distortion from $CsCu_2Cl_3$ to $CsCu_2Br_3$ to $CsCu_2I_3$, which could be used to explain the noticeable decrease in the PLQY for the iodide.[18] However, while the studies of octahedral connectivity and distortions have been useful for halide perovskites, more work is needed to ascertain the impact of the distortion of the coordination environment of Cu(I) on the optical properties of these new materials systems. We note here that it is especially difficult to tie PLQY to any single structural parameter as quenched PL may simply be due to lower crystallinity and/or higher defect concentration, differing impacts of defects on PL etc.

Table 1. Summary of Photoluminescence Properties of $CsCu_2X_3$[18]

Compound	PLQY (%)	FWHM (nm)	PLE (nm)	PL (nm)	CIE coordinates	CCT (K)	Stokes shift (nm)	Lifetime (ns)
$CsCu_2Cl_3$	48.0	102	319	527	(0.29, 0.52)	6437	208	13.8
$CsCu_2Cl_{1.5}Br_{1.5}$	0.37	200	340	587	(0.089,0.52)	12 577	247	15.1
$CsCu_2Br_3$	18.3	106	319	533	(0.27, 0.53)	6872	214	18
$CsCu_2Br_{1.5}I_{1.5}$	0.38	128	335	584	(0.48, 0.51)	3094	249	26.6
$CsCu_2I_3$	3.23	126	334	576	(0.43, 0.47)	3561	242	62

Since $CsCu_2X_3$ are STE-based mid-gap emitters, the origin of the PL peak shift and emission color change cannot simply be attributed to a rigid band shift. Instead, the careful analysis of the band structure reveals that VB and CB are largely similar in this family, and are predominantly derived from the Cu-3*d* and -4*s* orbitals, respectively.[21] This explains the unusual weak halogen dependence of PL in Cu(I) halides – unlike lead halide perovskites in which the valence band position is largely determined by halogen, the contribution of Cu orbitals dominates the states around the band gap. Therefore, the photoexcitation of $CsCu_2X_3$ promotes an electron into Cu-4s orbitals leaving a hole in Cu-3d orbitals. Notably, very similar band structures with Cu states dominating VB and CB have been reported for all other all-inorganic Cu(I) halides as well. Other groups have used the unique band structure of Cu(I) halides to explain their unusual optical properties. Thus, it has been proposed that photoexcitation creates a Jahn-Teller active $3d^9$ photoexcited state, which then efficiently undergoes excited-state structural reorganization (i.e., light induced distortion) that stabilizes the STE states leading to their unusually high emission efficiencies.[29] From our perspective, such explanations need further support as continued research on photoluminescent halides featuring variety of metal cations suggest that even non-Jahn-Teller metal cations (e.g., Sb^{3+}, In^{3+}, Mn^{2+}, Zn^{2+}, Cd^{2+} etc.) can also give materials with very high efficiency STE-based emissions.

A recent computational study of photoemission properties of $CsCu_2X_3$ suggests that upon photoexcitation, the energy of the excited electron is lowered by the displacements of adjacent Cu ions to enhance the mixing between their Cu-4s orbitals, which results in the formation of Cu-Cu bonds.[21] As a result, the hole is localized at Cu centers while the electron is distributed between the Cu atoms. The formation of Cu-Cu bonds in the $^1_\infty[Cu_2X_3]^-$ anionic double chains can happen via three distinct distortions that break Cu-X bonds, and the relative energies of the three STE states that are stabilized through such distortions are halogen dependent. The rationalization for the formation of different STE states corresponding to different structural distortions in $CsCu_2X_3$ can be tied to changes in the crystal structures upon halogen substitution; as just one example of the changes in interatomic distances, the increasing halide radii results in the increased Cu–Cu distance along the *c*-axis in the $^1_\infty[Cu_2X_3]^-$ anionic double chains from 2.80 Å in $CsCu_2Cl_3$ to 2.91 Å in $CsCu_2Br_3$ to 3.05 Å in $CsCu_2I_3$.[21] The formation energy of STEs via Cu-Cu formation along the *c*-axis, therefore, would be different in these three structures. This neatly explains the weak (but noticeable) halogen dependence of PL in $CsCu_2X_3$.[21] Furthermore, the reported STE binding energy values are starkly different for the three compounds in

this family, for example, binding energy of a similar STE state is reduced from 1.82 eV for $CsCu_2Cl_3$ to 1.25 eV for $CsCu_2Br_3$ to 0.34 eV for $CsCu_2I_3$. The proposed explanation for this trend is the change in ionicity in this family, that the more ionic $CsCu_2Cl_3$ shows stronger charge localization and exciton self-trapping, resulting in a larger exciton binding energy. Extending the conclusions of the original work by Du, we can attribute the much higher PLQY of $CsCu_2Cl_3$ in this family to its very high exciton binding energy, which leads to the presence of room temperature stable STEs in this material, and very high PLQY of 48%.[21] In fact, in our view, these computational results provide a much more robust explanation for the trends in PLQY as compared to the inspection of very small differences in tetrahedral distortions of $CsCu_2X_3$ based on X-ray diffraction work in their ground state (e.g., the tetrahedral bond distance variance values, Δd_{tet}, are very close, 21.67 10^{-4} for $CsCu_2Cl_3$, 13.59 10^{-4} for $CsCu_2Br_3$, and 3.05 10^{-4} for $CsCu_2I_3$).[18]

Notwithstanding the difficulty in relating ground state structural parameters to the observed optical properties, it is abundantly clear that the immediate environment around Cu has a significant impact on the observed photophysical properties. This fact was elegantly demonstrated by the study of structural and optical properties of $CsCu_2I_3$ under pressure (Figure 3 (c-d)). $CsCu_2I_3$ shows significant enhancement of emission due to pressure-induced structural changes; the crystal structure changes from the space group from *Cmcm* to the lower symmetry *Pbnm* group (Figure 3 (e)).[20] This phase transition involves a significant distortion of the Cu^IX_4 tetrahedra, which has been used to explain the slight changes in the PL peak position and a significant enhancement of PL emission intensity. Upon further compression, the PL intensity decreases due to the amorphization of the sample. Beyond $CsCu_2I_3$ itself, these results are significant and support the assignment of PL emission to STEs formation of which is impacted by local structural changes. From practical perspective, this experiment outlines a future research direction focused on PL emission switching in Cu(I) halides using pressure as an optical regulator.

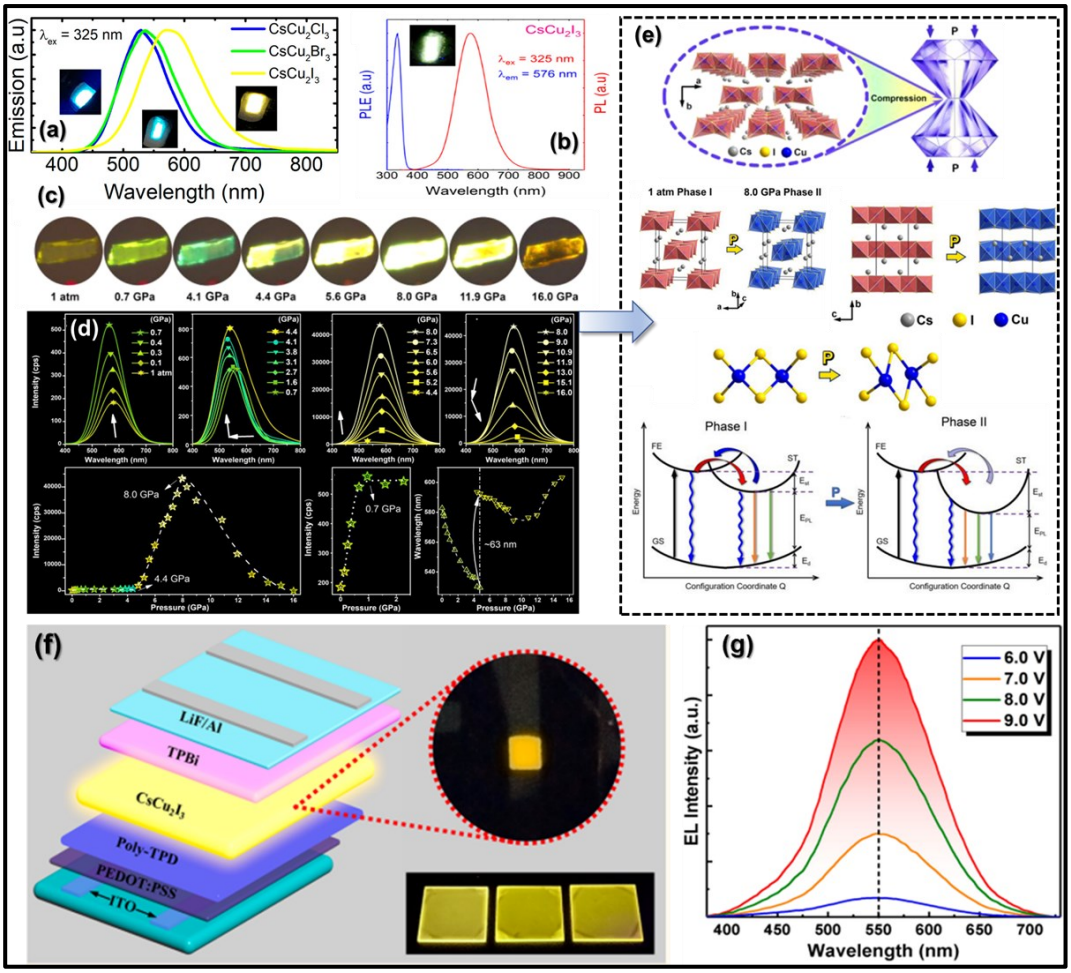

Figure 3. (a) Photoluminescence emission from $CsCu_2X_3$ (X = Cl, Br, I).[18] Reproduced from Ref 18. Copyright 2019 American Chemical Society. (b) PL excitation (blue, PLE) and emission spectra (red, PL) of $CsCu_2I_3$.[14] Reproduced from Ref 14. Copyright 2019 American Chemical Society. (c) Photoemission from $CsCu_2I_3$ under compression up to 16.0 GPa using excitation light source from 315 and 375 nm. (d) PL spectral changes for a $CsCu_2I_3$ crystal under compression up to 16.0 GPa. (e) Structural phase transition observed for $CsCu_2I_3$ under compression impacts the trapping and de-trapping processes of the excitons.[20] Reproduced from Ref 20. Copyright 2020 American Chemical Society. (f) Yellow-emitting LED prototype using $CsCu_2I_3$ as the emitting layer.[46] (g) Electroluminescence (EL) spectra of the device operated under various voltages of 6.0, 7.0, 8.0, and 9.0 V, respectively.[46] Reproduced from Ref 46. Copyright 2020 American Chemical Society.

Applications: In addition to the potential use in pressure sensing, yellow emitting $CsCu_2I_3$ has also been demonstrated to be a suitable alternate LED material to yellow-emitting lead halide perovskites, which suffer from stability issues at higher biases. The original report on $CsCu_2X_3$ reported a proof of principle device in which $CsCu_2I_3$ was used as an additive in a 1,3-bis(N-carbazolyl)benzene (mCP) host layer (the device structure of ITO/MoO_3/TAPC/mCP:$CsCu_2I_3$/TmPyPb/LiF/Al), yielding an external quantum efficiency (EQE) of ~0.1 %.[18] This study was followed by numerous others, which resulted in the significant increase in the device efficiency values. Thus, Ma et al. demonstrated a stable yellow LED using the $CsCu_2I_3$ emitting layer (Figure 3 (f-g) using the device structure of ITO/PEDOT:PSS/poly-TPD/$CsCu_2I_3$/TPBi/LiF/Al. The champion device achieved an EQE of 0.17 % and current efficiency of 0.46 cd/A. [46] The latter study attempted to use pristine $CsCu_2I_3$ as the emitter layer, and this is unlikely to yield devices with very high efficiencies as $CsCu_2I_3$ (and other Cu(I) halides reviewed here) have low crystal and electronic structure dimensionalities leading to very localized charges and poor carrier transport properties. Instead, the host-guest strategy used by us in our original report can alleviate the poor transport properties of Cu(I) halides by including them as additives to organic host layers. Indeed, a recent work has shown that inclusion of polyethylene glycol sorbitan monooleate (Tween) in the Cu(I) halide layer of the LED device ITO/poly (3,4-

ethylenedioxythiophene):poly (styrenesulfonate) (PEDOT:PSS, 30 nm)/metal halides (~60 nm)/1,3,5-Tri(m-pyridin-3-ylphenyl) benzene (TmPyPB, 45 nm)/lithium fluoride (LiF, 1 nm)/aluminum (Al, 100 nm) can provide peak EQE values of up to 3.1%.[47] Note that in this study, the metal halide emitter layer included both the yellow-emitting $CsCu_2I_3$ and blue-emitting $Cs_3Cu_2I_5$. Our own follow-up device work has shown that the host−dopant strategy used in OLEDs can give EQE value of 7.4% for the device structure of ITO/PEDOT:PSS/TAPC (15 nm)/TcTa (30 nm)/TcTa:TmPyPB:0.5% $CsCu_2I_3$ (30 nm)/TmPyPB (55 nm)/LiF/Al. The use of $CsCu_2I_3$ as an additive had two purposes: (i) overcome the poor charge transport properties of the pristine $CsCu_2I_3$ film, and (ii) increase the emission efficiency of the emitting layer (PLQY increases from 4.46% for the pristine $CsCu_2I_3$ film to 84.8% for the TmPyPB: 0.5% $CsCu_2I_3$ emitting layer). These results are notable not only because EQE of 7.4% is the record value for lead-free metal halide LEDs[48] but also shows that optical, electronic and charge transport properties of Cu(I) halides could be further improved through judicious device optimization efforts.

(b) The 213 family

In the A_2CuX_3 (A = K, Rb; X = Cl, Br) family, Rb_2CuX_3 were studied first and found to emit bright blue light under UV excitation due to STEs. The PL emission peaks are centered at 385 and 395 nm and PLQY values are measured to be 64 % and 100% for Rb_2CuBr_3 and Rb_2CuCl_3, respectively (Figure 4).[23] Although Rb_2CuCl_3 has a record high blue emission efficiency of 100%, it is reported to have markedly poor photostability and air stability, making its use in practical applications challenging. For better understanding of the photophysics of the system, electronic band structures and density of states (DOS) of Rb_2CuX_3 were studied. The valence band is mainly made up of Cu-3*d* orbitals hybridized with halogen *p* orbitals, while the conduction band has a mixed character of Cu-4*s* and halogen-*p* orbitals.[23] The STEs are found to be localized around the Cu ions in the 1D $[CuX_3]^{2-}$ chains. As is clear from the computational results, the band structures and exciton localization observed for the 213 family are largely similar to that of the 123 family. However, photoemission in the two families is starkly different based on the reported PL parameters; the 213 family PL peak positions are blue-shifted by 130-150 nm, the Stokes shift values are much less (< 100 nm), and FWHM values are also about twice less in the 213 family. The reported PL lifetimes are also about 3 orders of magnitude different, ns range lifetimes were reported for the 123 family whereas the 213 family has μs range lifetimes. The only similarity is in the PLE peak positions, which are in the UV range with a small difference of less than 20 nm. The latter confirms the fact that Cu-3*d* and -4*s* orbitals determine the bandgap in both families, but marked differences are present in the nature of STEs formed in the two families. Though both families are nominally 1D in terms of crystal structure dimensionality and are based on Cu^IX_4 tetrahedra, the difference in connectivity of these tetrahedra, i.e., the corner-sharing of Cu^IX_4 tetrahedra in Rb_2CuX_3 (*vs* edge-shared in $CsCu_2X_3$) leads to longer Cu–Cu distances, and the structural distortion leading to the formation of Cu–Cu bonds at the excited state is not energetically favored.[21] As a result, unlike $CsCu_2X_3$, Rb_2CuX_3 do not stabilize multiple kinds of STEs, instead, a single higher energy STE state is formed through trapping of excitons around Cu ions, which involves significant elongation of Cu – X bonds at the distortion sites.

After initial work on Rb_2CuX_3, our group further extended this family by synthesizing the isostructural K_2CuX_3.[7] Experimental optical studies revealed that the compounds are blue emitters with PL peaks around 390 nm (Figure 4(a)) with the reported PL parameters almost identical to that of Rb_2CuX_3. This suggests the insensitivity of emission properties of A_2CuX_3 to the changes on the A site. Indeed, the A site cations do not contribute to the states around the band gap (Figure 4(e)), and they evidently do not even indirectly impact the excited-state structural distortions that trap excitons. Therefore, the work on A_2CuX_3 clearly shows that these compounds are insensitive to substitutions of both halide anions and A cations, a significant departure from virtually every other metal halide family reported to date. The reported PLQY values of 96.58% for K_2CuCl_3 and 55% for K_2CuBr_3 are also among the highest in literature (Figure 4(c)). K_2CuCl_3 shows a long PL lifetime of 12.97 μs, which is typical for copper(I) halides (Figure 4(d), Table 2). Note that both in K_2CuX_3 and Rb_2CuX_3, the chloride

analogue has a higher PLQY value than the bromide. Extending the conclusions made for the 123 family based on computational studies that binding energy of STEs, and consequently, stability of STEs, depend on the ionicity of the bonds in the chains, could help explain this trend as well.[21] The chlorides with higher ionicity localize the charges better and stabilize STEs, leading to a more efficient STE-based emission.

Applications: The substitution studies in the A_2CuX_3 family not only provides a better fundamental understanding of Cu(I) halides but also has potential practical benefits. Thus, unlike Rb_2CuX_3, K_2CuX_3 show much improved photostability and air stability for around three weeks. In fact, our single crystalline K_2CuX_3 samples stored in air for months showed negligible degradation. One of the prospective applications of the A_2CuX_3 compounds is in scintillators for X-ray detection.[7,49,50,51] For this application, Rb_2CuX_3 are less desirable as they contain intrinsically radioactive Rb, and the photostability of Rb_2CuX_3 is notoriously poor with a rapid degradation within an hour under high energy irradiation.[7] Therefore, the more stable and Rb-free K_2CuX_3 are better choice. Multiple studies have confirmed that K_2CuX_3 single crystals display an intense radioluminescence when exposed to bremsstrahlung X-rays with a wavelength similar to the blue PL emission.[7] The reported light yield for K_2CuBr_3 is 23,806 photons per MeV, which is noticeably lower than the record high light yield of ≈91056 photons per MeV reported for Rb_2CuBr_3.[22] For scintillators heavier elemental composition (higher *Z*) is more advantageous for optimized X-ray attenuation efficiency, which explains the lower light yield value obtained for K_2CuBr_3. Nevertheless, it must be stressed that the light yield for K_2CuBr_3 is also among the highest, comparable to the traditional scintillator $Lu_{1.8}Y_{0.2}SiO_5$:Ce (24,900 photons/MeV).[51]

All-inorganic silver halides: The mechanism of degradation of Rb_2CuCl_3 involves oxidation of Cu(I) to Cu(II).[23] Therefore, we also attempted to improve the air stability of A_2CuX_3 by replacing copper with silver. A secondary important goal of this study was to bring tunability of PL to the "213" family – since the states around the bandgap are dominated by Cu orbitals, direct replacement of it with silver is expected to impact their electronic band structures. Yet a third goal of this substitution is the fact that A_2AgX_3 have higher *Z* than A_2CuX_3 counterparts, which could be advantageous for their potential radiation detection applications. To confirm these ideas, T. Creason et al. prepared A_2AgX_3 (*A* = Rb, Cs; *X* = Cl, Br, I), which were found to be broadband emitters with peak maxima ranging from 485 to 537 nm.[26] The PL profiles of A_2AgX_3 are characterized by very large Stokes shifts between 171 and 262 nm, leading to their significantly red-shifted emission peaks as compared to A_2CuX_3. In fact, the red-shifted broad emissions of Rb_2AgCl_3, Rb_2AgBr_3, Cs_2AgBr_3 and Cs_2AgI_3 appear as white light emission to a naked eye. Such stark changes are only partly due to the changes in crystal structures (discussed above), instead, they were attributed to the drastically different electronic structures and defect properties of silver halides. In terms of band structures, the bottoms of CBs are made of Ag-5*s* orbitals mixed with halogen orbitals. The Ag-4*d* states are more delocalized and contribute to the top of VBs, however, equally important contributors are halogen *p*-states (in case of Rb_2AgI_3, halogen contribution to VBM dominates). As a result, the band gaps change following the regular electronegativity trends from Rb_2AgCl_3, Rb_2AgBr_3, to Rb_2AgI_3, which is in agreement with the red shift of PL excitation energies observed in the experiments.

While the electronic band structures of A_2CuX_3 and A_2AgX_3 are markedly different, which can explain the trends in PLE, the large Stokes shifts suggest that A_2AgX_3 are also midgap emitters. The major additional difference between the two families is the fact that A_2AgX_3 are predominantly defect based emitters. Multiple studies suggest that Ag(I) halides may stabilize both defect-bound excitons (DBEs) and self-trapped excitons (STEs), contrary to the copper counterparts.[26, 28] For example, Rb_2AgBr_3 has two PL peaks, one narrower higher energy peak and a broad lower energy peak. In-depth computational studies and experimental defect formation/healing experiments suggest that the higher energy narrower peak originates from STEs, whereas the lower energy broad peak originates from DBEs, which are excitons bound to halogen vacancies. The attribution of the broad PL peak to DBEs

is further supported by the common knowledge of highly defective nature of silver halides, and annealing experiments done to manipulate defect properties of A_2AgX_3. Thus, a prolonged evacuation of a Rb_2AgBr_3 sample leads to a significant enhancement of the defect PL peak intensity.[28] Our own experiments on Rb_2AgI_3 suggest that its PL properties are highly dependent on the sample preparation history, with samples that are annealed for a short time showing predominantly STE emission. In contrast, longer annealing results in higher halogen vacancy concentration, leading to a dominant DBE-based emission. Such sample preparation history dependence of optical properties has not been observed for any reported Cu(I) family, which appear to be defect tolerant, and their reported optical properties have been consistent in tens of publications by different research groups.

Applications: Regarding the radiation detection properties of A_2AgX_3, a study reports that Rb_2AgBr_3 has a high light yield (25 600 photons MeV^{-1}), which is markedly lower than that of Rb_2CuBr_3. Despite its higher average *Z*, the light yield is lower for Rb_2AgBr_3 because of its much lower PLQY of 27%. In fact, the accurate measurement of PLQYs of A_2AgX_3 is quite difficult because of the extremely broad nature of their PL emission spectra. Nevertheless, the fact that A_2AgX_3 have much lower light emission efficiencies compared to A_2CuX_3 is visible to a naked eye. The obvious (but not fully confirmed!) explanation for the consistently lower PLQYs of A_2AgX_3 is the abundance of defects in Ag(I) halides, which could and do contribute to the observed PL emission but also act as centers of non-radiative recombination, lowering PLQYs. The discussed contrasting properties of A_2CuX_3 and A_2AgX_3 point to a significant gap in knowledge – the defect properties of many of the Cu(I) and Ag(I) have not been thoroughly studied. Future experimental and computational studies aimed at determining the dominant point defects in A_2CuX_3 and A_2AgX_3, their formation energies and the roles they play in their unique photophysical properties are welcome. For example, A_2CuX_3 show emission efficiencies up to 100% at room temperature – what are the dominant defect and their concentrations? Are these defects benign in A_2CuX_3? Yet another poorly understood phenomenon is the anti-Stokes photoluminescence (ASPL) property of Rb_2CuCl_3, reported for the first time by us (Figure 4 (b)).[23] We tentatively attributed ASPL to a phonon-assisted mechanism, and a recent study confirms this attribution based on their excitation wavelength-, excitation power-, and temperature-dependent ASPL spectra.[52] Further work on the ASPL properties of Cu(I) could shed light on the fundamental photophysics of these materials systems, and from practical perspective, could also enable solid-state refrigeration using A_2CuX_3 via laser cooling experiments.

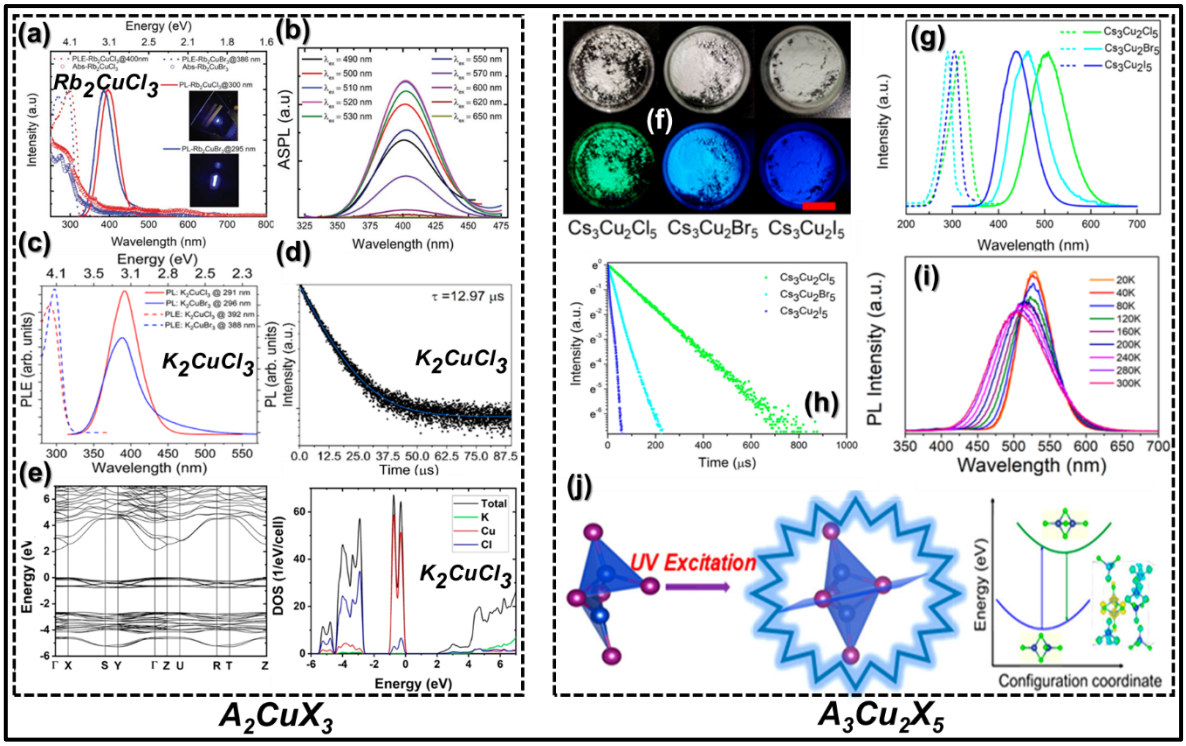

Figure 4. (a-e) Optical properties of the 213 family: (a) Room temperature optical absorption (circles), PLE (dashed lines) and PL (solid lines) of polycrystalline powders of Rb_2CuBr_3 (blue) and Rb_2CuCl_3 (red).[23] The insets show the bright blue emission under UV irradiation. (b) Anti-Stokes photoluminescence spectra of a Rb_2CuCl_3 single crystal measured at ambient temperature and for different excitation wavelengths. (c) Room temperature PLE and PL plots for K_2CuX_3. (d) Room-temperature PL lifetime decay plot for K_2CuCl_3. (e) Electronic band structure and DOS plots of K_2CuCl_3.[7] (f-j) Optical properties of the 325 family[33]: (f) Digital photograph of $Cs_3Cu_2X_5$ under ambient light (top) and ultraviolet light irradiation at 254 nm with a scale bar of 1 cm. (g) PLE and PL spectra of $Cs_3Cu_2X_5$ at room temperature.[33] (h) PL lifetime characteristics of $Cs_3Cu_2X_5$ at room temperature.[33] (i) Temperature dependence of PL for $Cs_3Cu_2Cl_5$.[33] (j) Schematic illustration portraying local distortion under photoexcitation which enhances the symmetry of the spindle-like $[Cu_2X_5]^{3-}$ dimers present in the $Cs_3Cu_2X_5$ crystal. Configuration coordinate diagram for the formation of STEs in $Cs_3Cu_2Cl_5$.[33] Reproduced from Ref 33. Copyright 2020 American Chemical Society.

(c) *The 325 family*

$Cs_3Cu_2X_5$ (X = Cl, Br, I) demonstrate high-efficiency blue and green light emission properties: the chloride is a green emitter, and substitution of chloride with heavier halides lead to blue shifting of PL (Figure 4 (f)).[33,29,14] $Cs_3Cu_2Cl_5$, $Cs_3Cu_2Br_5$ and $Cs_3Cu_2I_5$ display green, sky blue, and deep blue light emission under 254 nm UV irradiation with emission peaks around 515 nm, 461 nm, and 445 nm, respectively (Figure 4 (g)).[33] This trend in PL peak positions is contrary to the general trend observed in other metal halides (e.g., $CsPbX_3$) whose valence band positions are determined by the halogen states. Similar to the other Cu(I) halides, $Cs_3Cu_2X_5$ are STE-based midgap emitters, and therefore, the trends in PL can be attributed to the different structural deformations that stabilize STEs at different energy levels in the three compounds.[33] Although visually different, we note that the optical properties of $Cs_3Cu_2Br_5$ and $Cs_3Cu_2I_5$ are particularly similar: (i) the PL peak positions are less than 20 nm apart, (ii) PLE peak positions are around 15 nm apart, and (iii) consequently, the Stokes shift values are also similar. In contrast, the PL and PLE peak positions and Stokes shifts are considerably different for $Cs_3Cu_2Cl_5$. While the current explanation attributes the observed PL trends broad to differing band structures and excitonic properties in this family, as mentioned before (see section I), there remains questions about the particular polymorph of $Cs_3Cu_2Cl_5$ used in literature, i.e., whether the 1D $Cs_3Cu_2Cl_5$

type or the 0D $Cs_3Cu_2I_5$ type polymorph.[33] Therefore, more work is necessary to ascertain that the observed optical property differences are not simply due to the differing crystal structure of $Cs_3Cu_2Cl_5$.

Surprisingly, $Cs_3Cu_2Cl_5$ displays a temperature-dependent lifetime and red shifting in emission properties with a decrease in emission temperature (Figures 4 (h-i)). This indicates that the self-trapping barrier in these materials is low, and therefore, excitons get trapped easily. The reported lifetimes vary from single digit to double digit μs for $Cs_3Cu_2Br_5$ and $Cs_3Cu_2I_5$, to over 100 μs $Cs_3Cu_2Cl_5$, yet another stark difference of the chloride member. At present, the emissions from $Cs_3Cu_2X_5$ are attributed to the STEs that are localized on the dimeric $[Cu_2X_5]^{3-}$ unit. Our own computational work on $Cs_3Cu_2Br_5$ and $Cs_3Cu_2I_5$ suggests that the binding energies of excitons localized in the $[Cu_2X_5]^{3-}$ molecular anion are high, over 1 eV (after structural relaxation).[14] The modeled structural distortion breaks two Cu-X bonds and leads to the formation of elongated Cu–Cu bond, with holes localized on Cu centers and electrons localized between the two Cu centers. The coupling between the Cu $3d_z^2$ orbitals that form the Cu–Cu bond in the photoexcited state leads to a "local structure symmetrization", the $[Cu_2X_5]^{3-}$ unit in its photoexcited state is more accurately described as a face sharing tetrahedral dimer (Figure 4(j)).[33] Interestingly, the described structural reorganization that happens through the Cu–Cu bond formation in the photoexcited $Cs_3Cu_2X_5$ is similar to that observed for the 123 family. Unlike the 123 family, however, the 0D $Cs_3Cu_2X_5$ stabilize only one STE state since there is only one possible distortion that forms a Cu–Cu bond for exciton trapping in a $[Cu_2X_5]^{3-}$ unit. [21]

Electronic band structure calculations show that the VB and CB in $Cs_3Cu_2X_5$ are predominantly composed of Cu-3*d* and -4*s* orbitals, respectively.[14] The orbital make up of bands around the Fermi level and excited state structural distortions are similar to that in observed for the 123 family, however, the reported emission efficiencies are significantly higher for $Cs_3Cu_2X_5$. Up to unity PLQY (Table 2) has been reported for both $Cs_3Cu_2Cl_5$ and $Cs_3Cu_2I_5$, while $Cs_3Cu_2Br_5$ also shows high emission efficiency above 50%. While the PLQY varies tend to vary from sample to sample (depending on the preparation conditions and the measurement methods used by different groups), an attempt can be made to rationalize the differences in emission efficiencies based on the crystal structures of Cu(I) halides (see section I). Thus, the reason for differing emission efficiencies between the 123, 213 and 325 can perhaps be tied to the structural dimensionality arguments and different degrees of charge localization in these three families (the 123 family members have the most dispersive bands). However, these types of arguments and judgments largely remain qualitative in nature, and more work is necessary to tie the specifics of crystal structures to the resultant observed optical properties.

Applications: The very high PLQYs of $Cs_3Cu_2X_5$ suggests that they can be viable candidates for a number of applications. However, as mentioned above for the 123 family, the strong charge localization in $Cs_3Cu_2X_5$, which contributes to their observed high PLQYs, also results in poor charge transport properties. Nevertheless, there have been several attempts to use members of the 325 family in electronic applications. Jun et al. reported the fabrication of blue LED with the device structure of ITO/ZSO/$Cs_3Cu_2I_5$/NPD/MoO_x/Ag, which gave insufficient EL and maximum luminance of ≈10 cd m^{-2}.[29] In addition to the poor charge transport, the low performance of the device was attributed to the unoptimized energy level alignment; $Cs_3Cu_2I_5$ has a large band gap with the reported electron affinity (EA) of ≈2.7 eV and ionization potential (IP) of ≈6.5 eV. These values suggest that for LED applications, there are large barrier heights for the electron/hole injection and finding suitable contacts is difficult.[29] The use of $Cs_3Cu_2X_5$ as optical materials is less challenging. For example, the green emitting $Cs_3Cu_2Cl_5$ has been used in the fabrication of white LEDs (WLEDs) with very high color rendering (CRI) index by blending it with $BaMgAl_{10}O_{17}:Eu^{2+}$ (blue) and (Sr, Ca) $AlSiN_3:Eu^{2+}$ (red) phosphors on a 365 nm LED chip.[37] The fabricated UV-pumped WLEDs displayed a high CRI of 96 (R9 - 83 and R12 - 93) and CIE 1931 chromaticity coordinates of (0.357, 0.361), and a CCT of 4203 K. Both solution and melt processability of $Cs_3Cu_2I_5$ and its high stability are significant advantages for practical applications such as X-ray and γ-ray scintillators. Several recent studies reported Bridgman melt growth of $Cs_3Cu_2I_5$ and Tl-doped $Cs_3Cu_2I_5$ crystals.[53,54] The reported scintillation yields are high,

~32 000 photons MeV^{-1} under X-ray radiation and 29 000 photons MeV^{-1} under γ-ray radiation, which can be significantly enhanced through doping, the highest light yield to 98,200 photons/MeV obtained via Tl-doping far exceeds NaI:Tl, CsI:Tl, and $LaBr_3$:Ce scintillators. [30,55]

These encouraging examples of practical applications of $Cs_3Cu_2X_5$ open the door for further research: (i) a combination of copper(I) halide phosphors could be used to fabricate rare-earth free, environmentally friendly, inexpensive and high performance WLEDs with very high CRI values, and (ii) for scintillation radiation detection, further studies of optimized doping and crystal growth for improved performance. Other applications may also be considered such as remote thermometry and thermography, e.g., based on the high rate of change of the PL lifetimes with respect to temperature (e.g., the reported value of 2.7 μs/°C for $Cs_3Cu_2Cl_5$ is quite high).[33] The use of $Cs_3Cu_2X_5$ in radiation detection shows that doping can significantly improve their light yield, which points to another important future research direction – doping studies of all-inorganic Cu(I) halides are currently lacking, and they may provide fundamentally interesting and practically important results.

(d) ***Mixed anion family***

Alloying on the halide site has been successfully demonstrated both in the 123 and 325 families, which suggest that complete solid solutions can be made in the cases of $Cs_3Cu_2Br_{5-x}I_x$ ($0 \leq x \leq 5$) and $CsCu_2X_3$.[14, 18]Unlike these, the discovery of the mixed anion $Cs_5Cu_3Cl_6I_2$ suggests possibility of obtaining brand new line compounds and structure types in chloride iodide metal halide systems.[24] In the case of $Cs_5Cu_3Cl_6I_2$, the presence of iodide and chloride ions with differing sizes and electronic properties leads to unique 1D zigzag $^1_\infty[Cu_3Cl_6I_2]^{5-}$ chains, which stabilize STEs giving deep blue emission. The reported PL peak, Stokes shift and PLQY values of 462 nm, 191 nm and 95%, respectively, are similar to that of the 325 family (Table 2). Furthermore, other PL parameters such as the peak broadness and PL lifetime are also on par with that of the 325 family. The PL lifetime of $Cs_5Cu_3Cl_6I_2$ was found to increase when cooled, which is in contrast to the unchanging lifetime of $Cs_3Cu_2I_5$. These contrasting results suggest that $Cs_5Cu_3Cl_6I_2$ has a lower energy barrier for the thermal quenching process.

In terms of its electronic band structure, $Cs_5Cu_3Cl_6I_2$ is similar to the other alkali copper(I) halides, its valence band is made of hybridized Cu-3*d* and halogen *p* orbitals, and the conduction band is composed of mixed Cu-4*s* and halogen *p* orbitals. As is expected for low-dimensional Cu(I) halides with such orbital contributions, VB is quite flat, leading to very large effective mass of holes. It is proposed that upon photoexcitation, the holes are quickly localized around copper, which then bind excited electrons to form STEs. The easily deformable crystal lattice of Cu(I) halides aids the formation of STEs, leading to room temperature stable STEs that provide very high efficiency light emission upon recombination.[23,7] We note that specific deformation that traps excitons has not yet been reported for $Cs_5Cu_3Cl_6I_2$, therefore, immediate parallels with the other all-inorganic Cu(I) halides cannot be made (i.e., whether the deformations involve Cu–Cu bond formation). On the other hand, the advantageous characteristics of $Cs_5Cu_3Cl_6I_2$, such as low cost, nontoxic and nonradioactive elemental composition, high efficiency light emission etc. indicate that it is a candidate material for optical applications. In fact, $Cs_5Cu_3Cl_6I_2$ has been reported to show strong radioluminescence during powder X-ray diffraction experiments, suggesting its potential use in scintillators and X-ray imaging.[24]

Table 2. Summary of Optical Properties of All-inorganic Copper(I)/Silver(I) halides

Families	Compounds	$[Cu_nX_m]$ Structure	PLE (nm)	PL (nm)	FWHM (nm)	Stokes Shift (nm)	Lifetime (μs/ns)	PLQY (%)	Ref
"123"	$CsCu_2Cl_3$	edge-sharing	319	527	102	208	13.8 ns	48.0	[18]
	$CsCu_2Br_3$	tetrahedral	319	533	106	214	18.0 ns	18.3	
	$CsCu_2I_3$	chain	334	576	126	242	62.0 ns	3.23	

"213"	Rb_2CuCl_3	corner-	300	385	52	100	12.21 μs	100	[23]
	Rb_2CuBr_3	sharing	300	395	54	85		98.6	[22]
	K_2CuCl_3	tetrahedral	291	392	54	101	12.97 μs	96.58	[7]
	K_2CuBr_3	chain	296	388	54	92		55	[7]
"213"	Cs_2AgBr_3	corner-	285	537	-	233	58.82 μs	6.37	[26]
	Cs_2AgI_3	sharing	308	485	-	171	14.67 μs	14.41	[26]
	Rb_2AgCl_3	tetrahedral	275	537	-	262	0.62 μs	-	[26]
	Rb_2AgBr_3	chain	283	485	-	202	0.77 μs	1.52	[26]
	Rb_2AgI_3		304	485	-	181	1.15 μs	0.37	[26]
"325"	$Cs_3Cu_2Cl_5$	dimers	275	510	95	235	109 μs	99	[24]
	$Cs_3Cu_2Br_5$	formed by	298	455	75	157	1.41 μs	50.07	[24]
	$Cs_3Cu_2I_5$	edge-sharing tetrahedral	309	443	99	135	0.46–0.56 μs	98.7	[24]
	$Cs_3Cu_2Br_{3.75}I_{1.25}$	and trigonal	293	456	85	164	-	53.8	[14]
	$Cs_3Cu_2Br_{2.5}I_{2.5}$	planar units	294	453	89	159	-	55.2	[14]
	$Cs_3Cu_2Br_{1.25}I_{3.75}$		300	448	93	148	-	60.4	[14]
"Mixed anion"	$Cs_5Cu_3Cl_6I_2$	1D zig-zag tetrahedral chain	271	462	95	191	40 μs	95	[24]

3. Hybrid organic-inorganic copper(I) halides

Despite the advantageous characteristics of all-inorganic copper(I) halides including low-cost, rare-earth free, earth abundant and nontoxic elemental composition, ease of processing via solid-state and wet chemistry methods, and record high light emission efficiencies, some of them suffer from poor air stability, and most of them suffer from a lack of tunability of their optical properties. Consequently, preparation and fundamental characterization of hybrid organic-inorganic Cu(I) halides is one of the emerging research directions that could address these significant drawbacks. The substitution of *A*-site cation in alkali copper(I) halides with an organic cation has no known limits as the target Cu(I) halides are low-dimensional (typically 0D or 1D, and 2D in very rare cases), and therefore, no clearly outlined size and shape parameters exist (e.g., such as the restrictions imposed by the tolerance factor for halide perovskites).[9] Therefore, hybrid Cu(I) halides with essentially unlimited structural diversity promise endless possibilities in terms of investigations of the crystal structure-optical property relationships in emissive Cu(I) halides. In addition to the fundamental materials discovery and structure-property trends, targeted work in this area is likely enable the control over light emission properties of resultant materials, bring tunability in PL emission, and lead to an enhancement of stability.[56]

Our own ongoing work in this area can be divided into 3 directions: (i) using organic cations of various sizes and shapes for targeted preparation of 0D and 1D structures, (ii) influencing the coordination environment and polyhedral distortions around individual Cu centers, e.g., by employing organics with differing H-bonding capabilities, and (iii) using photoactive organic molecules to bring PL tunability. Our structural analyses show clear differences between alkali Cu(I) halide families based on their structural dimensionality (1D *vs* 0D), connectivity of polyhedral units (corner- *vs* edge-sharing) and density of packing of the polyanionic units. Therefore, controlled preparation of Cu(I) halides with target structures using custom design organics of various sizes and shapes in which structural trends can easily be tied to the trends in optical properties is an important future area of research. The use of organics with different H-bonding capabilities is *hypothesized* to be important for controlling the degree of structural distortion around Cu centers, and consequently, impacting the structures and optical properties of hybrid copper(I) halides. This idea is supported by the fact that narrow structural variations in the $CsCu_2X_3$ leads to the stabilizations of different STE states and that PL is much enhanced by the local distortion of Cu polyhedral in $CsCu_2I_3$. [20, 21] Finally, incorporation of luminescent organic molecules could lead to unique interactions between organic and inorganic luminescence centers, perhaps even dual band emission profiles that can provide full spectral tunability of PL in this new

materials class. In addition to the targeted structural templating and PL property changes, the incorporated organics could be designed to provide enhanced air, moisture, and thermal stability.

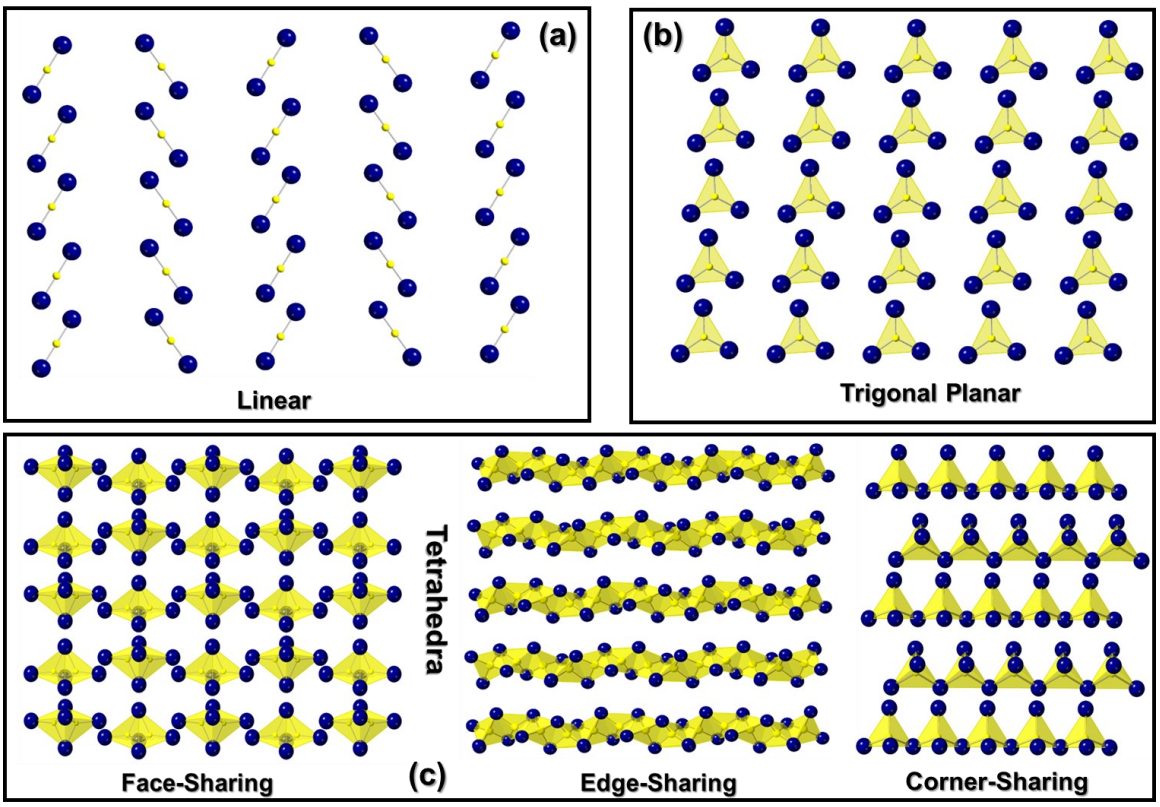

Figure 5. Schematic diagram showcasing structural diversity found in copper(I) halides featuring different structural building units (a) linear, (b) trigonal planar, (c) tetrahedral units with different connectivity modes (face-sharing, edge-sharing and corner-sharing tetrahedra) that can be templated by suitable choice of organic cations.

Recent publications on hybrid organic-inorganic copper(I) halides seem to confirm the validity of the above-proposed approach. The replacement of alkali cations K^+, Rb^+ and Cs^+ with larger organic cations is expected to increase the distances between $[Cu_nX_m]^{z-}$ polyanionic units in the resultant hybrid copper(I) halides.[57] Furthermore, the specific size and shape characteristic of the selected organic cations can alter the connection modes of copper halide tetrahedra forming structures based on corner-sharing, edge-sharing, and face-sharing (Figure 5).[58, 59] Unlike the *p*-block metals, copper is known for having different types of environments in its compounds including tetrahedral, trigonal planar, and linear coordination environments (Figure 5). [7, 23, 60, 61,62,] Since alkali copper(I) halide structures are based on tetrahedral $[CuX_4]$ building blocks, perhaps the first question is if non-tetrahedral Cu(I) halides are also luminescent. With this question in mind, we prepared and characterized $(Ph_4P)MX_2$ (Ph_4P^+ = tetraphenylphosphonium; M = Cu, Ag; X = Cl, Br), which exhibit 0D crystal structures featuring isolated linear $[CuX_2]^-$ and dimeric $[Ag_2Cl_4]^{2-}$ anions made of edge-sharing approximate trigonal planar units.[63] The utilization of the bulky Ph_4P^+ cations ensure the complete isolation of inorganic molecular anions with the nearest distances between the metal centers in isolated anions higher than 7.1 Å. However, despite the maximized charge localization, $(Ph_4P)MX_2$ are found to be rather weak light emitters with the estimated PLQY values of ~1%. On the other hand, $(TBA)CuBr_2$ (TBA^+ = tetrabutylammonium) containing linear $[CuBr_2]^-$ units embedded periodically in the matrix of TBA^+, displays a bright broadband cyan emission with a high PLQY of 55%.[64] Another publication on $(TBA)CuCl_2$ and $(TBA)CuBr_2$ with the same structure reports even higher PLQY values of 92.8% and 80.5 % with emission peaks at 510 nm and 498 nm, respectively.[60] These results suggest that the quenched PL observed for $(Ph_4P)MX_2$ cannot simply be attributed to their non-tetrahedral crystal

structures as linear $[CuX_2]^-$ containing $(TBA)CuX_2$ are high-efficiency emitters. Instead, the dramatic change in the electronic structure of $(Ph_4P)MX_2$ is responsible for the quenched PL. Our computational work shows that the inorganic molecular anions in this family, $[CuX_2]^-$ and $[Ag_2X_4]^{2-}$, have large band gaps of ~4 eV, and the organic Ph_4P^+ cations form midgap states within the inorganic gap. This unique electronic structure indicates that upon photoexcitation, a spatial separation of excited electrons and holes occur, which results in markedly lower PL efficiency in $(Ph_4P)MX_2$. These conclusions are further supported by a recent study on an unrelated compound $PyCs_3Cu_2Br_6$ (Py^+ = pyridinium), which has a 0D crystal structure based on trigonal planar $[CuBr_3]$ building blocks.[59] $PyCs_3Cu_2Br_6$ is also reported to be non-emissive due to the due to the spatial separation of the excited electron and hole on organic and inorganic structural units, respectively. In contrast, the reported electronic structure of the high-efficiency cyan light emitter $(TBA)CuBr_2$ is similar to that of blue emitting alkali Cu(I) halides, with the VBM deriving predominantly from Cu-3*d* orbitals with some Br-4*p* mixing and the CBM composed mainly of Br-4*p* and Cu-4*s* states.[64,60] These results indicate that the relative alignments of organic and inorganic band gaps in hybrid Cu(I) halides should be considered for the design of high efficiency emitters (i.e., type I alignment in which both localized either on the organic or inorganic component is preferred). However, note here that contradicting literature reports on the band alignment of Cu(I) halides exist. For example, $(TBA)CuI_2$ is also known in literature, but it contains $[Cu_2I_4]^{2-}$ dimers formed by edge sharing CuI_3 trigonal planar units and therefore should perhaps be more accurately referred to as $(TBA)_2Cu_2I_4$. This compound displays dual-band white-light emission with a high PLQY of 54.3%.[56] However, unlike $(TBA)CuCl_2$ and $(TBA)CuBr_2$, the VBM and CBM of $(TBA)_2Cu_2I_4$ are reported to include hybridized Cu-3*d* and I-5*p* orbitals and organic molecular orbitals, respectively. Based on our knowledge, the relatively low partial density of Cu-4*s* states can be easily missed, therefore, a careful inspection of CBM for $(TBA)_2Cu_2I_4$ will likely reveal the dominant contribution of dispersive Cu-4*s* states (DOS will be rather low), similar to that in *all* other highly emissive Cu(I) halides.

Beyond the changes in PL efficiency, interesting is the fact that the green/cyan emissions of $(TBA)CuX_2$ with PL peaks ranging from 498 to 510 nm constitute a significant red-shift compared to the blue emission demonstrated by the all-inorganic Cu(I) halides with 0D structure, $Cs_3Cu_2Br_5$ and $Cs_3Cu_2I_5$. Instead, the reported PLE_{max}, PL_{max}, Stokes shifts, FWHM values and lifetimes in tens-hundreds of microseconds for $(TBA)CuX_2$ are very similar to that of the green emitting $Cs_3Cu_2Cl_5$, for which more careful work is needed to ascertain its crystal structure-optical property relationship. In our view, these results suggest that structure and chemistry of both hybrid and all-inorganic Cu(I) halides impact the observed optical properties, but more work is needed to clarify these connections. While $Cs_3Cu_2Cl_5$ and $(TBA)CuX_2$ have similar optical properties, one added benefit of the hybrid materials is the fact that they are reported to display superior stability against water even when soaked for 24 hours. $(TBA)CuBr_2$ was found to have higher thermal stability than $(TBA)CuCl_2$, as they showed no degradation until 240 °C while the $(TBA)CuCl_2$ started to degrade after 70 °C followed by a large degradation step at 250 °C.[60] The improved stability is attributed to a highly regular arrangement of water-resistant TBA^+ cations which sterically isolate $[CuBr_2]^-$ units.[64]

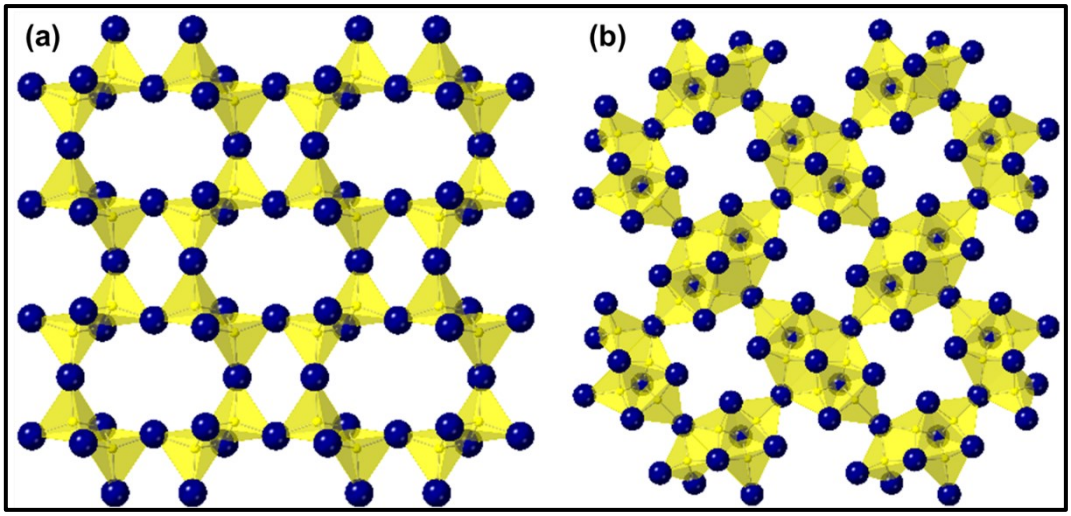

Figure 6. Top views of the unique 2D polyanionic layers in the structures (a) $(t\text{-}BA)_2Cu_2I_4{\cdot}H_2O$ and (b) $(t\text{-}BA)_3Cu_6I_9$.

The use of bulky organic cations with non-linear shapes may yield unique structure types such as in the case of $(t\text{-}BA)_3Cu_6I_9$ ($t\text{-}BA^+$ = tert-butyl-ammonium), which reportedly is not luminescent but quickly degrades in air displaying moisture-induced green photoluminescence properties.[65] The non-luminescent $t\text{-}BA_3Cu_6I_9$ crystallizes in the tetragonal space group *P*4*bm* featuring a novel 2D layered crystal structure. [65]The crystal structures of Cu(I) halides mentioned so far are all either 1D or 0D in terms of crystal structure dimensionality, and the fact that Cu(I) halides can form 2D layered structure is a significant result. The authors report that six $[CuI_4]$ tetrahedra share common edges to form $[Cu_6I_9]^{3-}$ structural units which in turn share corners to form the 2D layered crystal structure (Figure 6). This compound reacts with moisture present in the air and producing a degradation product with a bright green emission peak at 520 nm and a high PLQY of 59.4%. The degradation product was separately obtained by growing crystals in the presence of water, which yielded another new compound, $(t\text{-}BA)_2Cu_2I_4{\cdot}H_2O$. The authors write that transformation between non-emissive $t\text{-}BA_3Cu_6I_9$ and green emitting $(t\text{-}BA)_2Cu_2I_4{\cdot}H_2O$ is reversible through moist air exposure of the former and heating at 100 °C for the latter. This reversibility is preserved even after 50 cycles, which suggests that the material system could be used as a low-cost moisture sensor.[65] More important from fundamental perspective, the hydrate $(t\text{-}BA)_2Cu_2I_4{\cdot}H_2O$ is also reported to have a 2D layered crystal structure made of edge- and corner-sharing $[CuI_4]$ tetrahedra. On the basis of the very strong electron-phonon coupling in $(t\text{-}BA)_2Cu_2I_4{\cdot}H_2O$, as evidenced by the high Huang–Rhys factor of ~90, the authors attributed green emission to STEs. Since both $(t\text{-}BA)_3Cu_6I_9$ and its degradation product $(t\text{-}BA)_2Cu_2I_4{\cdot}H_2O$ have 2D crystal structures, and the calculated electronic structures for them are also largely similar (with the VBM and CBM largely derived from Cu and I), question remains as to why one is non-emissive whereas the other one has a very high PLQY, and the original publication does not provide a clear and conclusive answer. It is also noteworthy that despite their 2D crystal structures, VB qualitatively looks as flat as that reported for 1D and 0D copper(I) halides, which could explain the unexpectedly high PLQY of 59.4% for $(t\text{-}BA)_2Cu_2I_4{\cdot}H_2O$. As for the comparison between the two 2D layered Cu(I) halides, the authors proposed that $(t\text{-}BA)_2Cu_2I_4{\cdot}H_2O$ has a higher degree of charge localization based on computational results. Based on our own inspection of the isosurface plots of wave function $|\Psi|^2$ of CBM and VBM, an excited state structural reorganization that forms Cu – Cu bond seems quite possible for the dimeric $[Cu_2I_4]$ structural units, similar to the ones published for alkali Cu(I) halides. However, why this is not possible for the hexameric $[Cu_6I_9]^{3-}$ structural units should be studied further.

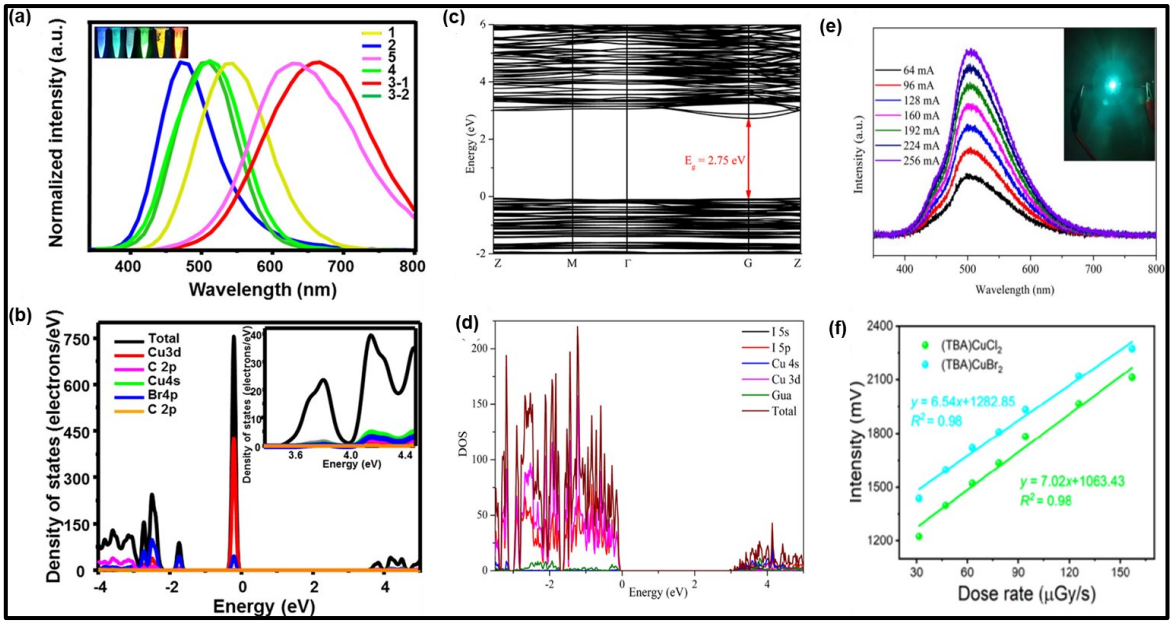

Figure 7. (a) PL spectra of different hybrid copper bromides whose emission in the visible region (from blue to orange-red) is controlled by tuning organic cation chain length. Inset: photographs of the corresponding powder samples under 254 nm UV light $(TMA)_3Cu_2Br_5$ **(1);** $(TEA)_2Cu_2Br_4$ **(2);** $(TPA)_2Cu_4Br_6$ **(3-1);** $(TPA)CuBr_2$ **(3-2);** $(TBA)CuBr_2$ **(4);** $(TBA)_2Cu_4Br_6$ **(5)**.[66] [Reproduced from Ref 66. Copyright [2019] American Chemical Society] (b) Density of state plot for **(3-1)**. (c) Band structure and (d) density of state plots for $(Gua)_3Cu_2I_5$.[61, 67] (e) Emission spectra of a 310 nm UV pumped LED based on $(Gua)_3Cu_2I_5$ powders with different driving currents.[67] [Reproduced from Ref 67. Copyright [2021] American Chemical Society] (f) The X-ray response intensity of $(TBA)CuCl_2$ and $(TBA)CuBr_2$ single crystals as a function of dose rate.[60] Reproduced from Ref 60. Copyright 2021 American Chemical Society.

Structural and coordination environment changes in copper(I) bromides can be induced by using organic cations of different chain lengths, such as that demonstrated by using tetraalkylammonium bromides with different alkyl chains (Figure 8).[66] Six different 0D Cu(I) bromide structures have been reported using tetramethylammonium (TMA^+), tetraethylammonium (TEA^+), tetrapropylammonium (TPA^+) and tetrabutylammonium (TBA^+) as the organic cations in $(TMA)_3Cu_2Br_5$, $(TEA)_2Cu_2Br_4$, $(TPA)_2Cu_4Br_6$, $(TPA)CuBr_2$, $(TBA)CuBr_2$, and $(TBA)_2Cu_4Br_6$ (Figure 7). Of these, $(TMA)_3Cu_2Br_5$, $(TEA)_2Cu_2Br_4$, $(TPA)_2Cu_4Br_6$ and $(TBA)_2Cu_4Br_6$ are based on a trigonal planar $[CuBr_3]$ building block, whereas $(TPA)CuBr_2$ and $(TBA)CuBr_2$ contain linear $[CuBr_2]$ units. While the cyan/green emission of $(TBA)CuBr_2$ has already been discussed above, the optical properties of $(TPA)CuBr_2$ are almost identical with the PL peak position of 507 nm, PLQY of 83%, and lifetime in hundreds of μs. Therefore, just like in the case of the $(TBA)CuX_2$ family, light emission in $(TPA)CuBr_2$ can be attributed to STEs localized on $[CuBr_2]^-$ units with no interference from the organic cation. Particularly interesting is the case of $(TMA)_3Cu_2Br_5$, which has a component ratio matching that of the $A_3Cu_2X_5$ family, yet its structure is markedly different, $[Cu_2Br_5]^{3-}$ anions are formed by two corner-sharing trigonal planar $[CuX_3]$ units. Consequently, the observed optical properties of $(TMA)_3Cu_2Br_5$ are also distinct.[66] Another important conclusion from this work is that although emission in all six compounds has been attributed to STEs localized on $[Cu_nBr_m]$ units, the changes in crystal structures helped achieve emission color tunability in a broad range from blue to orange-red, i.e., 476 nm to 664 nm with very high PLQYs up to 97% (Table 3, Figure 7 (a), Figure 8).[66] In addition, particularly promising finding is the fact that Cu(I) bromides featuring same polyanionic clusters such as the members of the $(R)CuX_2$ or $(R)_2Cu_4Br_6$ (R = organic cation) families have close lying PL emission peaks, which indicates a degree of predictability of PL properties based on the polyanionic structures. Nevertheless, important contribution of organic cations to the deformability of crystal lattice cannot be ignored, e.g., differing lattice rigidities could explain the PL_{max} shift of ~40 nm between $(TPA)_2Cu_4Br_6$ and $(TBA)_2Cu_4Br_6$.

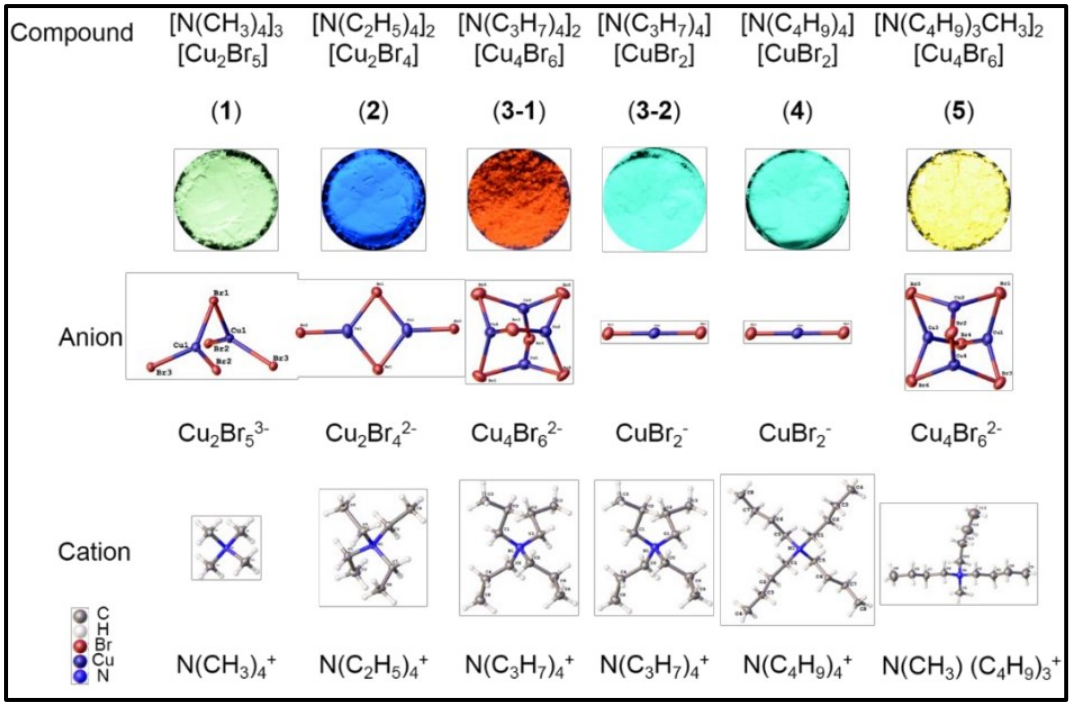

Figure 8. Powder samples of $(TMA)_3Cu_2Br_5$ (1), $(TEA)_2Cu_2Br_4$ (2), $(TPA)_2Cu_4Br_6$ (3-1), $(TPA)CuBr_2$ (3-2), $(TBA)CuBr_2$ (4), and $(TBA)_2Cu_4Br_6$ (5) under 254 nm UV light, and the respective anionic inorganic motifs and cationic motifs in their crystal structures.[66] Reproduced from Ref 66. Copyright 2019 American Chemical Society.

Table 3. Photophysical Properties of Quaternary Ammonium Cu(I) Bromides[66]

Compounds	λ_{max} (nm)	Emission color	CIE	PLQY (%) (λ_{ex}/nm)	Lifetime (μs)
$(TMA)_3Cu_2Br_5$	542	Yellow	(0.35, 0.51)	91 (315)	80.70
$(TEA)_2Cu_2Br_4$	476	Blue	(0.18, 0.25)	91 (317)	53.53
$(TPA)_2Cu_4Br_6$	664	Orange red	(0.53, 0.43)	97 (386)	39.04
$(TPA)CuBr_2$	507	green	(0.20, 0.40)	83 (254)	248.98
$(TBA)CuBr_2$	504	green	(0.22, 0.40)	97 (254)	11.99
$(TBA)_2Cu_4Br_6$	623	Yellow orange	(0.50, 0.45)	2 (365)	41.73

Further evidence of the effect of the arrangement of copper halide units on the emission properties of hybrid copper halides can be found in another recent report on $(Gua)_3Cu_2I_5$ (where Gua = guanidinium, $CH_6N_3^+$). The DOS and band structure of $(Gua)_3Cu_2I_5$ have been studied to gain photophysical insights (Figure 7 (c)-(d)). While the crystal structure of $(TMA)_3Cu_2Br_5$ differs from that of the $Cs_3Cu_2X_5$ family, $(Gua)_3Cu_2I_5$ containing face-sharing $[Cu_2I_5]^{3-}$ dimers is structurally analogous to the 0D $Cs_3Cu_2I_5$ type structure. The compound emits cool white light with 96 % PLQY; it also displays reversible thermo-induced luminescence, i.e., its PL emission can be tuned back and forth between cool-white (PL_{max} ~ 500 nm) and yellow (PL_{max} = 548 nm) emission through heating/cooling cycles between 300–370 K.[67] Temperature-dependent PL studies suggest that $(Gua)_3Cu_2I_5$ is a dual band STE-based emitter including two independent shallow and deep STE states. These observations are in stark contrast to the reported blue emission due to the single STE state stabilized in $Cs_3Cu_2I_5$, even though there is a publication reporting dual band emission for $Cs_3Cu_2I_5$ as well.[68] However, the report

of dual band emission in $Cs_3Cu_2I_5$ is yet to be confirmed, and in the particular case of $Cs_3Cu_2I_5$, great care must be taken to ensure the highest degree of sample purity as the yellow emission peak reported in $Cs_3Cu_2I_5$ may simply be due to the presence of the yellow-emitting impurity $CsCu_2I_3$. In fact, the authors of the $(Gua)_3Cu_2I_5$ study report that the emission change from cool-white to yellow upon heating is due to a structural phase transition based on PXRD results, raising an important question if yellow-emitting $(Gua)Cu_2I_3$ is formed in the process. Notwithstanding the unexplained nature of the phase transition of $(Gua)_3Cu_2I_5$, the authors' referral to a study on $Cs_3Cu_2I_5$ reporting *simultaneous* dual band blue and yellow emission seems misplaced – $(Gua)_3Cu_2I_5$ has a blue emission with similar PL parameters to that of the structurally analogous $Cs_3Cu_2I_5$ at room temperature. The relatively small differences in PL properties between $(Gua)_3Cu_2I_5$ and $Cs_3Cu_2I_5$ could be attributed to the difference in the $[Cu_2I_5]^{3-}$ dimers, which are based on face-sharing tetrahedra in the former and edge-sharing tetrahedron and trigonal planar unit in the latter (i.e., they are distorted versions of one another). In addition to the high temperature phase transitions, the authors of the study on $(Gua)_3Cu_2I_5$ also discuss the observed dual band emission between 80–300 K, which in our view requires further supporting evidence. For example, computational results showing the two different and stable STE states in such small $[Cu_2I_5]^{3-}$ dimers would help. What kinds of distinct excited state structural reorganizations occur in this case? It is our understanding that the stabilization of two distinct STE states on such a small anionic molecule would be difficult. Indeed, another comparable size tetrahedral dimer, $[Cu_2Br_6]^{4-}$, made of corner-sharing tetrahedra also shows only a single STE-based green emission peak in $(MA)_4Cu_2Br_6$. Its bright broadband green emission at 524 nm (understandably shifted due to the different structure of the dimer) is characterized by PLQY of 93%.[69] In fact, our own past experience on $Cs_3Cu_2I_5$ is such that we had samples that showed dual band yellow and blue emissions, which prompted us to do more experimental work leading to the discovery of the yellow-emitting $CsCu_2I_3$ and rest of the $CsCu_2X_3$ family. For these reasons, we believe that more work on $(Gua)_3Cu_2I_5$ and its derivatives is warranted to confirm and understand the dual band emission between 80–300 K, and to determine the nature of the structural phase transition between 345–360 K.

Stabilization of multiple STE states in 0D hybrid Cu(I) halides have also been reported for $(C_8H_{24}N_4)Cu_2X_6{\cdot}4H_2O$ (CuX-en) (X = Cl, Br) and $(C_{10}H_{28}N_4)Cu_2X_6$ (CuX-am) (X = Cl, Br, I).[70] In CuX-en and CuX-am, two adjacent tetrahedra are sharing common edges to form $[Cu_2X_6]^{4-}$ dimers, similar to the $[Cu_2Br_6]^{4-}$ dimers in $(MA)_4Cu_2Br_6$. In contrast to the green emission at 524 nm demonstrated by $(MA)_4Cu_2Br_6$ (Table 4), the emission of CuX-en and CuX-am range from blue (450 nm) to orange (565 nm). The authors report that while CuX-am has regular PL spectra that can be fit with a single Gaussian function, the PL spectra feature broader peaks for CuX-en, which can only be fit with double-Gaussian functions. This is then used as a basis for arguing presence of two STE states in photoexcited CuX-en. This study points to an important omission in literature – the unusual PL peak shapes for Cu(I) halides are scarcely mentioned or studied and may point to important clues relating to the PL mechanisms in this materials class. This is in part because of the difficulties associated with the measurements of broadband emitters with PL peaks covering almost entire visible spectrum. Nevertheless, attempt has been made to distinguish the two excitonic states in CuX-en as one-center a-STE (localized on Cu^+) and two-center m-STE (localized on Cu_2^{2+} dimer). Assuming that all samples are free of impurities, the two STE states in CuX-en can be judged as arising from slight variations in the excited state structural distortions that occur in these compounds.[70,21] Given our own experience in Cu(I) halides and arguments provided above, we think more justification is needed to argue in support of the possible stabilization of multiple STE states in very small molecular anionic units (e.g., with one or two tetrahedral units). To clarify this issue, a comprehensive study of PL peak shapes and parameters that impact them (e.g., impurities, defects, strain effects, measurement artifacts etc.) is necessary. Notwithstanding the existing gap in knowledge in this area, we must note here that the two STE emission centers under one broadband peak reported for CuX-en are distinctly different from the argued dual band emission in $Cs_3Cu_2I_5$ and $(Gua)_3Cu_2I_5$, for which the emission peaks are well separated (by

~100 nm or more). The latter would suggest the presence of very different structural distortions with similar formation energies and with similar trapping rates of excitons.

Table 4. Photoemission Characteristics of Hybrid Cu(I) Halides

Compounds	PLE (nm)	PL (nm)	Lifetime (µs)	FWHM (nm)	PLQY (%)	Ref.
$(TEA)_2Cu_2Br_4$	317	476 (Blue)	53.53		91	[66]
$(MA)_4Cu_2Br_6$	302	524 (green)	120	107	93	[69]
$(TBA)CuCl_2$	286	510 (green)	28.70	86	92.8	[60]
$(PEA)_4Cu_4I_4$	370	598 (Orange-red)	6.35	112	68%	[71]
$(TBA)CuI_2$	357	476 & 675 (White broad emission)	6.70		54.3	[56]
$(Gua)_3Cu_2I_5$	324	481 (cool white-at room temperature)	1.98	125	96	[67]
$(Ph_4P)CuCl_2$	304	562 (yellow)	-	-	~1	[63]
$(Ph_4P)CuBr_2$	294	526 (greenish yellow)	-	-	~1	[63]

Applications: The use of functional organics in the design of copper(I) halides for targeted applications is currently in its infancy. A recent study reports preparation of two chiral hybrid organic-inorganic copper(I) halides (R-/S-MBA)$CuBr_2$, which demonstrate promising nonlinear optical (NLO) properties with a highly efficient second harmonic generation (SHG) response, outstanding optical transparency, and high laser-induced damage thresholds (LDTs).[72] Highly emissive chiral Cu(I) halides can also be used for circularly polarized luminescence applications (e.g., in LEDs, anticounterfeiting, bioencoding) as demonstrated by work on (R/S-MBA)$_4Cu_4I_8 \cdot 2H_2O$ and acentric $Gua_6Cu_4I_{10}$. [73] Interestingly, these two compounds were discovered following the work on $(Gua)_3Cu_2I_5$ but have noticeably lower PLQYs around 21-22%. More on the application front, just like alkali Cu(I) halides, hybrid Cu(I) halides are also good candidates for phosphor applications. For example, Lian et al. demonstrated UV pumped white LED with high color rendering index of 78 using $(TBA)_2Cu_2I_4$.[56] Using $Gua_3Cu_2I_5$ as a phosphor, Song et al. prepared a cool-white light emitting UV-pumped LED that works in the 5.5 to 7.5 V range (Figure 7 (e)).[67] Despite encouraging proof-of-concept device performance, environmental, thermal and photostability of hybrid Cu(I) halides need further improvements to achieve spectrally stable photoemission for solid-state lighting applications. In addition to solid-state lighting, hybrid Cu(I) halides are also promising for radiation detection applications.[60] For example, $(TBA)CuCl_2$ and $(TBA)CuBr_2$ are reported to demonstrate high light yields of ~24,134 photons/MeV and 23,373 photons/MeV, respectively (Figure 7(f)).[60,74,70,75,76]

4. Unified mechanism of light emission in all-inorganic and hybrid Cu(I) halides

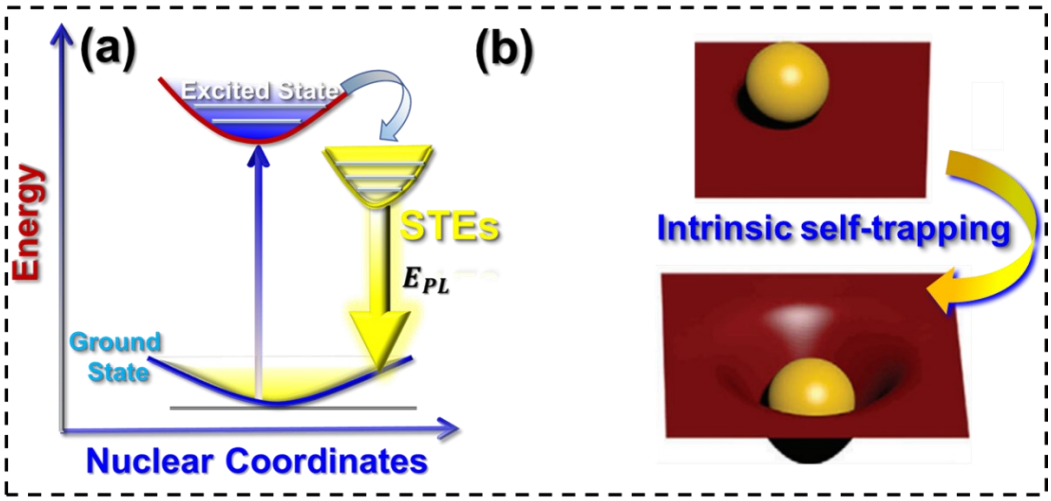

Figure 9. (a) Hybrid and all-inorganic Cu(I) halides emit light with record high efficiencies due to STE recombination. (b) Schematic representation of a self-trapped exciton formation.[77,78] Reproduced from Refs 77 and 78. Copyright 2018 American Chemical Society.

All-inorganic and hybrid organic-inorganic copper(I) halides belong to the larger family of low-dimensional metal halides displaying broadband and largely Stoke-shifted emission properties. This is in stark contrast to the parent 3D perovskites such as $CsPbX_3$, which are reported to show much narrower band edge emissions due to free exciton recombination. To summarize the existing body of work on Cu(I) halides, efficient light emission occurs for compounds whose VBM and CBM have predominant contributions from Cu-3*d* and Cu-4*s* orbitals, respectively, with some minor halide *p* orbital contributions to both. This conclusion is consistent across families of hybrid organic-inorganic and all-inorganic Cu(I) halides featuring very different structures based on linear $[CuX_2]$, trigonal planar $[CuX_3]$, and tetrahedral $[CuX_4]$ building blocks. If organic cations contribute to the bands around the Fermi level (typically to the CBM in the existing literature reports so far) to form type II band alignment, the PL is quenched in the resultant hybrid Cu(I) halides. The Ag analogues of hybrid Cu(I) halides invariably have much worse light emission efficiencies, often completely quenched PL (based on our published and yet unpublished results), presumably due to their significantly more defective nature. For the emissive hybrid Cu(I) halides, PL emission ranges are similar if the inorganic polyanions are identical, however, since the emissions are predominantly due to mid gap STE states, some variations exist (Figure 9 (a)-(b)).[79] This can be attributed to the differing degrees of lattice rigidity/deformability depending on the specific choices of organic counter cations, which then can lead to variations in the excited state structural distortions that trap excitons. Therefore, while on one hand there is some predictability of the resultant optical properties based on crystal structure information, on the other hand, the predictions are rather qualitative in nature with lower precision levels than desired. Notwithstanding the challenges in structural and property predictions, the ongoing work on hybrid Cu(I) halides brought tunability of PL emission, as originally hypothesized by us and others. But more work is needed to bring tunability of PLE spectra as most hybrid halides still require the more expensive UV photoexcitation. Whether a radical shift of PLE to blue range is possible is an open question, perhaps even doubtful, since the highly emissive Cu(I) halides all have optical transitions localized on isolated inorganic $[Cu_nX_m]$ units with band gaps between mostly Cu-3*d* and Cu-4*s* orbitals.

5. Future research directions

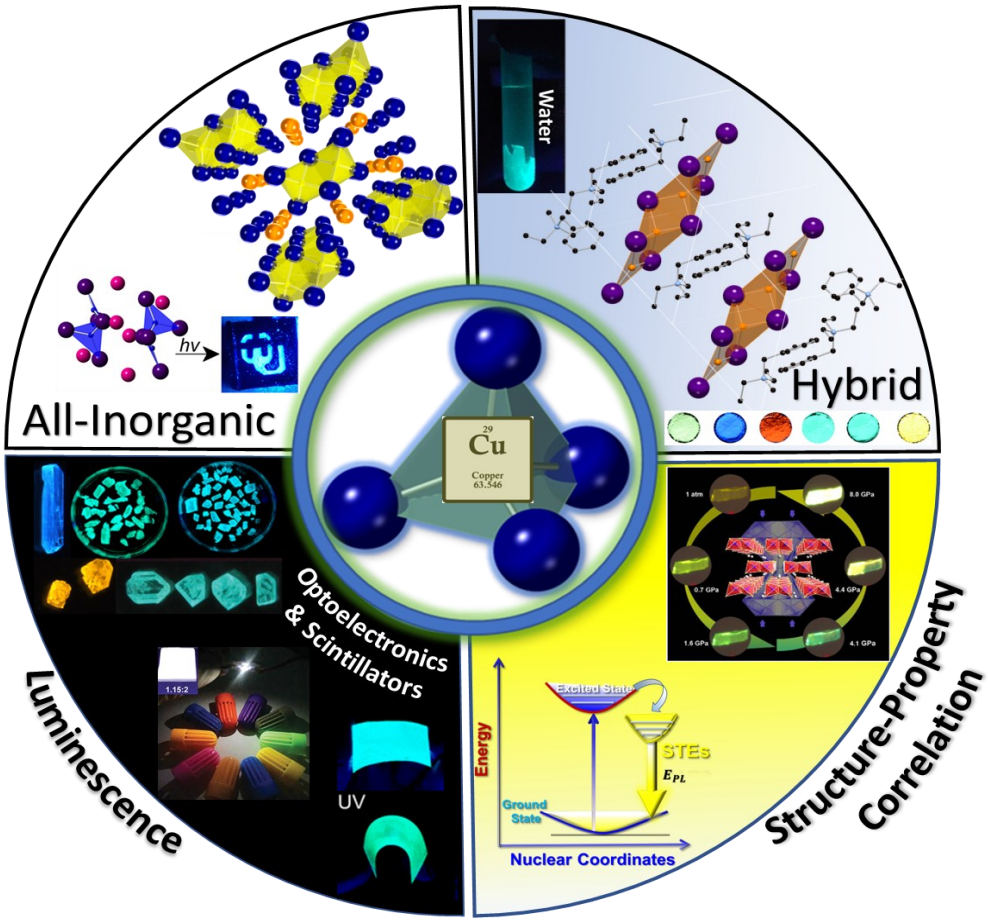

Figure 10. All-inorganic and hybrid organic-inorganic copper(I) halides with growing chemical and structural diversity are excellent STE-based light emitters, which allows their consideration for a myriad of optical and electronic applications and fundamental structure-property studies. Reproduced from Ref 14. Copyright 2019 American Chemical Society. Reproduced from Ref 66. Copyright 2019 American Chemical Society. Reproduced from Ref 64. Copyright 2021 American Chemical Society. Reproduced from Ref 60. Copyright 2021 American Chemical Society. Reproduced from Ref 20. Copyright 2020 American Chemical Society.

In this perspective, we have highlighted the progress made in understanding the fundamental structure-property correlation in all-inorganic and hybrid copper halides, along with the discussions on their contrasting photophysical properties and several of their potential applications (Figure 10). Throughout the perspective, we highlighted remaining questions and yet unaddressed challenges in the field. In addition to those, provided below are some possible key future research directions in this area:

- **Preparation of copper(I) halides with desired structures:** Synthetic solid-state chemistry is notorious for its lack of predictability, and the grand challenge of preparing crystalline materials with target structures is also applicable for inorganic and hybrid metal halides. Our structure-property analysis shows that the observed optical properties of Cu(I) halides are highly dependent on the intricacies of their crystal structures including metal coordination numbers, degrees of distortion of metal halide coordination polyhedra, their connectivity modes, and even their packing density. Therefore, if the goal is to prepare custom design light emitters based on Cu(I), very fine control over their crystal structures is needed. To date, the work on Cu(I) halides has been largely exploratory with both high temperature solid-state and solution phase self-assembly syntheses leading to unexpected

structures. For example, a number of compounds have been obtained with $RCuX_2$ compositions (R = organic cation; X = Cl, Br, I) but with very different crystal structures based on $[CuX_2]^-$ linear anions, $[CuX_3]^{2-}$ trigonal planar units that share common edges to form $[Cu_2X_4]^{2-}$ dimers, $[CuX_4]^{3-}$ tetrahedra that share edges and corners to form $[Cu_2X_4]^{2-}$ 2D layers. The reason for the presence of very different coordination polyhedra in Cu(I) halides is unknown beyond broad attribution of these observation to optimized packing in each of these cases. What is the role of the organic cation in stabilization of linear $[CuX_2]^-$, trigonal planar $[CuX_3]^{2-}$ and tetrahedral $[CuX_4]^{3-}$ building blocks? How can organic cations be controllably used to template 0D, 1D and 2D crystal structures? Besides these, the role of different organics in tuning the STE characteristics of Cu(I) halides (emission wavelength, trapping depth etc.) is neither well-documented nor understood fundamentally. Therefore, while the wealth and variety of structures displayed by Cu(I) halides provides an exciting playground for synthetic materials chemists, more systematic studies are required to achieve predictive synthesis of Cu(I) halides for fundamental studies. To this end, our group is currently conducting spectroscopic studies aimed at recognizing the optical fingerprints of different metal halide polyanions during the growth phase of crystals in the solution medium.[80] Additional concomitant studies are needed to explore new synthesis routes, build synthesis-crystal structure-optical property maps, and ultimately, to develop Cu(I) halide materials design methodologies.

- **Mechanistic studies of light emission in hybrid and alkali Cu(I) halides:** All-inorganic and hybrid organic-inorganic Cu(I) halide families reviewed in this perspective have all been reported as STE-based emitters. The mechanistic assignment of emission to STEs is often based on a combination of largely Stokes-shifted broadband emission, linear power-dependence of PL, temperature dependence of PL, typically long lifetimes in μs, and a few recent transient absorption (TA) spectroscopy studies. Given the large number of recent publications on Cu(I) halides with corroborating evidence for STE emission, the assignment of PL emission to trapped excitons is likely correct for most Cu(I) halide families. Yet, in our view, important questions remain about the nature of STEs in Cu(I) halides (regarding distortions that stabilize them, phonons involved in their formation, triplet *vs* singlet etc.). The distortions that trap excitons in Cu(I) halides with tetrahedral structures are understood better than the reported STEs in structures based on $[CuX_3]$ trigonal planar and particularly $[CuX_2]$ linear units. The propensity of tetrahedral $[CuX_4\}$ structures to excited state distortions is related to Jahn-Teller effect in literature (this needs more evidence), however, highly emissive linear CuX_2 molecules are not Jahn-Teller active, i.e., how and why would linear CuX_2 units distort upon photoexcitation?
  In addition, the published PL parameters sometimes vary for different structural families. For examples, the PL lifetimes displayed by $CsCu_2X_3$ range from 13 to 62 ns, contrary to most all-inorganic copper halides with up to hundreds of μs lifetimes.[18] Such large variations in PL parameters including lifetimes are also reported for other low-dimensional non-Cu halides demonstrating high efficiency PL. If all these compounds are STE-based emitters, do such large variations in lifetimes fit the proposed emission mechanism? Similarly, temperature-dependent PL measurements show negative thermal quenching of PL for a number of Cu(I) halides, i.e., upon cooling to cryogenic temperatures, the PL is quenched (e.g., for the Rb_2CuX_3 family). This result supports the STE assignment of the PL emission as the STE formation through lattice distortions requires phonons. On the other hand, for $CsCu_2X_3$, the integrated PL intensity is reported to decrease upon cooling and then saturate at 100 K.[18] In our work, we explained this observation using the Shibata model, yet these variations in temperature-dependent PL properties lead to important questions about the broad attribution of emission in Cu(I) halides to STEs.[18] In fact, deviating from the dominant STE emission assignment in literature, a recent study attributes PL emission in $Cs_3Cu_2I_5$ and $CsCu_2I_3$ to iodine vacancies. [81] This study points to

a key deficiency in literature, defect-based emission in Cu(I) halides has not been strongly considered as a possible alternative emission mechanism for the most part. Often, the linear dependence of PL intensity with increasing excitation power is used to rule out contribution from permanent defects, and indeed, defect-based emission intensity is expected to saturate upon increasing the excitation intensity. However, there is always a question if the measurements were stopped before saturation is reached, and in metal halides, researchers may limit the excitation power to their instrument capability and/or to ensure the material is not decomposed during the measurements. Therefore, both computational and experimental studies of defect properties of Cu(I) halides are urgently needed. Even if defect-based emission is ruled out, the fact that compounds such as $Cs_3Cu_2I_5$ have ~100% emission efficiency at room temperature suggests a need for in-depth studies of photophysical and defect properties of Cu(I) halides. What is the defect concentration in high-efficiency light emitting Cu(I) halides and why do they not act as centers of non-radiative recombination? Note here that in-depth studies of defect properties may also be helpful for understanding the reported anti-Stokes PL properties of Rb_2CuX_3. Our own yet unpublished work suggests that in several all-inorganic Cu(I) halide families, exciton self-trapping is highly efficient leading to largely immobilized STEs that do not move around the crystal lattice, and therefore, do not encounter defects, which are visible in optical spectra at cryogenic temperatures.

Custom-design Cu(I) halides for practical applications: Cu(I) halides are bright light emitters with emission efficiencies that rival or even surpass that of the state-of-the-art inorganic phosphors such as the blue phosphor $KMg_4(PO_4)_3:Eu^{2+}$.[82] However, stability of Cu(I) halides in air, photostability and thermal stability all need to be improved for long-term practical application considerations. This is particularly true for their proposed application in solid-state lighting – the commercial LEDs are advertised as lighting devices with long lifetimes in tens of years, and therefore, even though some of the Cu(I) halide families reviewed here have improved stability (as compared to other Cu(I) halides and lead halide perovskites), their long terms stability under device operation conditions needs to be studied. Yet another challenge is the fact that most Cu(I) halides are excited by UV radiation necessitating the use of expensive UV LED chips as compared to the more affordable blue 450 nm LED chips. To obtain full spectral tunability of PL and to shift PLE peaks to blue from UV, more targeted studies of hybrid Cu(I) halides are needed as the inclusion of organics seem to be effective in red shifting the emission; however, PLE peaks are still in the UV region for the hybrids reported to date, necessitating further optimization work. Additional doping studies may also be considered, particularly Cu-site engineering can be a way forward for optimizing the materials' optical properties. Furthermore, highly luminescent $[Cu_nX_m]$ units can be incorporated in heterometallic halide crystal structures containing other luminescent metal halide centers (e.g., red or green emitting $[Mn_nX_m]$) to construct families of single component white light emitters that can be viable alternatives to multicomponent inorganic phosphors, which reportedly suffer from self-absorption, different degradation profiles of different phosphors causing unusual shifts in emission colors etc. Note here, however, that the incorporation of Cu(I) halides into LEDs is not straightforward as they are typically broadband emitters (as are all STE-based emitters with strong electron-phonon coupling). In contrast, the current industry needs for various phosphors for solid-state lighting are focused on color pure narrow-band emitters. Therefore, the use of single component white light emitters or multiple broadband emitting Cu(I) halide phosphors in white LEDs (WLEDs) will require a completely different device design and optimization work, with follow-up tests for performance comparisons with the current state-of-the-art WLEDs. In the short term, the applications of bright emitting Cu(I) halides are more likely in radiation detection, where larger crystals can be encapsulated to

prevent degradation, and in niche applications such as data encryption and anticounterfeiting.

In summary, all-inorganic and hybrid copper(I) halides have synergistic combination of very high photoluminescence efficiencies, earth-abundant, nontoxic, and inexpensive elemental compositions, and low-cost processibility via wet chemistry and high temperature synthesis. These characteristics make Cu(I) halides viable candidates for a number of optoelectronic applications such as solid-state lighting, sensing (chemical, radiation, heat, temperature, etc.) and anti-counterfeiting. Much has already been accomplished in synthesis, characterization, and applications of Cu(I) halides in recent years and more exciting studies to address the remaining unanswered questions and practical challenges are expected in the coming years.

Biographies

Dhritiman Banerjee

Dhritiman Banerjee is currently pursuing his postdoctoral study at the University of Oklahoma. He received his MSc in Applied Physics and PhD in Physics from the Indian Institute of Technology (Indian School of Mines), Dhanbad, India in 2014 and 2020, respectively. Before joining the University of Oklahoma as a postdoctoral fellow in the Department of Chemistry and Biochemistry in 2021, Dr. Banerjee worked as an assistant professor in the Department of Physics at C. V. Raman Global University, Bhubaneswar, India (2020-2021). His research interest at present is focused on the design and development of novel hybrid copper/silver halides, their characterization and in-depth study of their photophysical properties for optoelectronics and security applications.

Bayram Saparov

Bayram Saparov is an Associate Professor of Chemistry at the University of Oklahoma. He received his Diploma in Chemistry from Lomonosov Moscow State University in 2006 and his Ph.D. in Inorganic Solid-State Chemistry from the University of Delaware in 2011. Before joining the University of Oklahoma as an Assistant Professor of Chemistry in 2016, Dr. Saparov was a postdoctoral researcher at Oak Ridge National Laboratory (2011-2014), and a Department of Energy (DOE) Energy Efficiency and Renewable Energy (EERE) SunShot Postdoctoral Fellow at Duke University (2014-2016). Dr. Saparov's group is currently interested in design, discovery, and characterization of multinary metal halides and chalcogenides for optical and electronic applications.

Acknowledgements

This work was supported by the National Science Foundation through the Faculty Early Career Development Program (NSF DMR-2045490).

References

(1) Li, X.; Gao, X.; Zhang, X.; Shen, X.; Lu, M.; Wu, J.; Shi, Z.; Colvin, V. L.; Hu, J.; Bai, X.; Yu, W. W.; Zhang, Y. Lead-Free Halide Perovskites for Light Emission: Recent Advances and Perspectives. *Adv. Sci.* **2021**, *8* (4), 2003334.

(2) Yan, F.; Tan, S. T.; Li, X.; Demir, H. V. Light Generation in Lead Halide Perovskite Nanocrystals: LEDs, Color Converters, Lasers, and Other Applications. *Small* **2019**, *15* (47), 1902079.

(3) Chen, J. K.; Zhao, Q.; Shirahata, N.; Yin, J.; Bakr, O. M.; Mohammed, O. F.; Sun, H. T. Shining Light on the Structure of Lead Halide Perovskite Nanocrystals. *ACS Materials Lett.* **2021**, *3* (6), 845-861.

(4) Protesescu, L.; Yakunin, S.; Bodnarchuk, M. I.; Krieg, F.; Caputo, R.; Hendon, C. H.; Yang, R. X.; Walsh, A.; Kovalenko, M. V. Nanocrystals of Cesium Lead Halide Perovskites ($CsPbX_3$, X = Cl, Br, and I): Novel Optoelectronic Materials Showing Bright Emission with Wide Color Gamut. *Nano Lett.* **2015**, *15* (6), 3692-3696.

(5) Slayney, A. H.; Smaha, R. W.; Smith, I. C.; Jaffe, A.; Umeyama, D.; Karunadasa, H. I. Chemical Approaches to Addressing the Instability and Toxicity of Lead-Halide Perovskite Absorbers. *Inorg. Chem.* **2017**, *56* (1), 46-55.

(6) McCall, K. M.; Morad, V.; Benin, B. M.; Kovalenko, M. V. Efficient Lone-Pair-Driven Luminescence: Structure-Property Relationships in Emissive 5s(2) Metal Halides. *ACS Mater Lett* **2020**, *2* (9), 1218-1232.

(7) Creason, T. D.; McWhorter, T. M.; Bell, Z.; Du, M.-H.; Saparov, B. K_2CuX_3 (X = Cl, Br): All-Inorganic Lead-Free Blue Emitters with Near-Unity Photoluminescence Quantum Yield. *Chem. Mater.* **2020**, *32* (14), 6197-6205.

(8) Koh, T. M.; Shanmugam, V.; Schlipf, J.; Oesinghaus, L.; Muller-Buschbaum, P.; Ramakrishnan, N.; Swamy, V.; Mathews, N.; Boix, P. P.; Mhaisalkar, S. G. Nanostructuring Mixed-Dimensional Perovskites: A Route Toward Tunable, Efficient Photovoltaics. *Adv Mater.* **2016**, *28* (19), 3653-3661.

(9) Saparov, B.; Mitzi, D. B. Organic-Inorganic Perovskites: Structural Versatility for Functional Materials Design. *Chem. Rev.* **2016**, *116* (7), 4558-4596.

(10) Willett, R.; Place, H.; Middleton, M. Crystal structures of three new copper(II) halide layered perovskites: structural, crystallographic, and magnetic correlations. *J. Am. Chem. Soc.* **1988**, *110* (26), 8639-8650.

(11) Slavney, A. H.; Hu, T.; Lindenberg, A. M.; Karunadasa, H. I. A Bismuth-Halide Double Perovskite with Long Carrier Recombination Lifetime for Photovoltaic Applications. *J. Am. Chem. Soc.* **2016**, *138* (7), 2138-2141.

(12) McClure, E. T.; Ball, M. R.; Windl, W.; Woodward, P. M. Cs_2AgBiX_6 (X = Br, Cl): New Visible Light Absorbing, Lead-Free Halide Perovskite Semiconductors. *Chem. Mater.* **2016**, *28* (5), 1348-1354.

(13) Meyer, G. NEUE CHLOR-ELPASOLITHE VOM TYP $CS_2AGLNCL_6$ (LN= SC, Y, CE-ND, SM-LU). **1977**.

(14) Roccanova, R.; Yangui, A.; Nhalil, H.; Shi, H.; Du, M.-H.; Saparov, B. Near-Unity Photoluminescence Quantum Yield in Blue-Emitting $Cs_3Cu_2Br_{5-x}I_x$ ($0 \leq x \leq 5$). *ACS Appl. Electron. Mater.* **2019**, *1* (3), 269-274.

(15) Manser, J. S.; Christians, J. A.; Kamat, P. V. Intriguing Optoelectronic Properties of Metal Halide Perovskites. *Chem. Rev.* **2016**, *116* (21), 12956-13008.

(16) Cenzual, P. V. K. Pearson's Crystal Data: Crystal Structure Database for Inorganic Compounds (on DVD). *ASM International: Materials Park* **2022/2023**.

(17) Brink, C.; van Arkel, A. R. The crystal structures of $(NH_4)_2CuCl_3$ and $(NH_4)_2CuBr_3$. *Acta Crystallogr.* **1952**, *5* (4), 506-510.

(18) Roccanova, R.; Yangui, A.; Seo, G.; Creason, T. D.; Wu, Y.; Kim, D. Y.; Du, M.-H.; Saparov, B. Bright Luminescence from Nontoxic $CsCu_2X_3$ (X = Cl, Br, I). *ACS Materials Lett.* **2019**, *1* (4), 459-465.

(19) Lin, R. C.; Guo, Q. L.; Zhu, Q.; Zhu, Y. M.; Zheng, W.; Huang, F. All-Inorganic $CsCu_2I_3$ Single Crystal with High-PLQY (approximate to 15.7%) Intrinsic White-Light Emission via Strongly Localized 1D Excitonic Recombination. *Adv.Mater.* **2019**, *31* (46), 1905079.

(20) Li, Q.; Chen, Z. W.; Yang, B.; Tan, L.; Xu, B.; Han, J.; Zhao, Y. S.; Tang, J.; Quan, Z. W. Pressure-Induced Remarkable Enhancement of Self-Trapped Exciton Emission in One-Dimensional $CsCu_2I_3$ with Tetrahedral Units. *J. Am. Chem. Soc.* **2020**, *142* (4), 1786-1791.

(21) Du, M. H. Emission Trend of Multiple Self-Trapped Excitons in Luminescent 1D Copper Halides. *ACS Energy Lett.* **2020**, *5* (2), 464-469.

(22) Yang, B.; Yin, L. X.; Niu, G. D.; Yuan, J. H.; Xue, K. H.; Tan, Z. F.; Miao, X. S.; Niu, M.; Du, X. Y.; Song, H. S.; Lifshitz, E.; Tang, J. Lead-Free Halide Rb_2CuBr_3 as Sensitive X-Ray Scintillator. *Adv.Mater.* **2019**, *31* (44), 1904711.

(23) Creason, T. D.; Yangui, A.; Roccanova, R.; Strom, A.; Du, M. H.; Saparov, B. Rb_2CuX_3 (X = Cl, Br): 1D All-Inorganic Copper Halides with Ultrabright Blue Emission and Up-Conversion Photoluminescence. *Adv. Opt. Mat* **2019**, *8* (2), 1901338.

(24) Li, J.; Inoshita, T.; Ying, T.; Ooishi, A.; Kim, J.; Hosono, H. A Highly Efficient and Stable Blue-Emitting $Cs_5Cu_3Cl_6I_2$ with a 1D Chain Structure. *Adv. Mater.* **2020**, *32* (37), 2002945.

(25) Jun, T.; Handa, T.; Sim, K.; Iimura, S.; Sasase, M.; Kim, J.; Kanemitsu, Y.; Hosono, H. One-step solution synthesis of white-light-emitting films via dimensionality control of the Cs–Cu–I system. *APL Mater.* **2019**, *7* (11), 111113.

(26) Kumar, P.; Creason, T. D.; Fattal, H.; Sharma, M.; Du, M. H.; Saparov, B. Composition-Dependent Photoluminescence Properties and Anti-Counterfeiting Applications of A_2AgX_3 (A = Rb, Cs; X = Cl, Br, I). *Adv. Funct. Mater.* **2021**, *31* (48), 2104941.

(27) Creason, T. D.; Fattal, H.; Gilley, I. W.; McWhorter, T. M.; Du, M.-H.; Saparov, B. $(NH_4)_2AgX_3$ (X = Br, I): 1D Silver Halides with Broadband White Light Emission and Improved Stability. *ACS Mater. Au* **2021**, *1* (1), 62-68.

(28) Zhang, M.; Wang, X.; Yang, B.; Zhu, J.; Niu, G.; Wu, H.; Yin, L.; Du, X.; Niu, M.; Ge, Y.; Xie, Q.; Yan, Y.; Tang, J. Metal Halide Scintillators with Fast and Self-Absorption-Free Defect-Bound Excitonic Radioluminescence for Dynamic X-Ray Imaging. *Adv. Funct. Mater.* **2021**, *31* (9), 2007921.

(29) Jun, T.; Sim, K.; Iimura, S.; Sasase, M.; Kamioka, H.; Kim, J.; Hosono, H. Lead-Free Highly Efficient Blue-Emitting $Cs_3Cu_2I_5$ with 0D Electronic Structure. *Adv. Mater.* **2018**, *30* (43), 1804547.

(30) Yuan, D. S. Air-Stable Bulk Halide Single-Crystal Scintillator $Cs_3Cu_2I_5$ by Melt Growth: Intrinsic and Tl Doped with High Light Yield. *ACS Appl. Mater. Interfaces* **2020**, *12* (34), 38333-38340.

(31) Zhang, X. T.; Zhou, B. A.; Chen, X. P.; Yu, W. W. Reversible Transformation between $Cs_3Cu_2I_5$ and $CsCu_2I_3$ Perovskite Derivatives and Its Anticounterfeiting Application. *Inorg. Chem.* **2022**, *61* (1), 399-405.

(32) Grandhi, G. K.; Viswanath, N. S. M.; Cho, H. B.; Han, J. H.; Kim, S. M.; Choi, S.; Im, W. B. Mechanochemistry as a Green Route: Synthesis, Thermal Stability, and Postsynthetic Reversible Phase Transformation of Highly-Luminescent Cesium Copper Halides. *J. Phys. Chem. Lett.* **2020**, *11* (18), 7723-7729.

(33) Lian, L. Y.; Zheng, M. Y.; Zhang, P.; Zheng, Z.; Du, K.; Lei, W.; Gao, J. B.; Niu, G. D.; Zhang, D. L.; Zhai, T. Y.; Jin, S. Y.; Tang, J.; Zhang, X. W.; Zhang, J. B. Photophysics in $Cs_3Cu_2X_5$ (X = Cl, Br, or I): Highly Luminescent Self-Trapped Excitons from Local Structure Symmetrization. *Chem. Mater.* **2020**, *32* (8), 3462-3468.

(34) Mykhalichko, B. M.; Davydov, V. N.; Aksel'rud, L. G. Synthesis and structure of $Cs_3Cu_2Cl_5$. *Russ. J. Inorg. Chem.* **1997**, *42* (7), 1011-1013.

(35) Sebastia-Luna, P.; Navarro-Alapont, J.; Sessolo, M.; Palazon, F.; Bolink, H. J. Solvent-Free-Synthesis and Thin-Film Deposition Of Cesium Copper Halides with Bright Blue Photoluminescence. *Chem. Mater.* **2019**, *31* (24), 10205-10210.

(36) Hull, S.; Berastegui, P. Crystal structures and ionic conductivities of ternary derivatives of the silver and copper monohalides—II: ordered phases within the $(AgX)_x$–$(MX)_{1-x}$ and $(CuX)_x$–$(MX)_{1-x}$ (M=K, Rb and Cs; X=Cl, Br and I) systems. *J. Solid State Chem.* **2004**, *177* (9), 3156-3173.

(37) Bai, W.; Shi, S.; Lin, T.; Zhou, T.; Xuan, T.; Xie, R.-J. Near-Unity Cyan-Green Emitting Lead-Free All-Inorganic Cesium Copper Chloride Phosphors for Full-Spectrum White Light-Emitting Diodes. *Adv. Photonics Res.* **2021**, *2* (3), 2000158.

(38) Sebastia-Luna, P.; Navarro-Alapont, J.; Sessolo, M.; Palazon, F.; Bolink, H. J. Solvent-Free Synthesis and Thin-Film Deposition of Cesium Copper Halides with Bright Blue Photoluminescence. *Chem. Mater.* **2019**, *31* (24), 10205-10210.

(39) Shen, D.; Wang, X.; Zhang, X.; Liu, Y.; Shi, Y.; Li, X.; Chen, X.; Zhang, Y. Real-Time Observation of Anion-Exchange Reaction in $Cs_3Cu_2Cl_5$ Single Crystal. *ACS Appl. Opt. Mater.* **2022**, *1* (1), 435–441.

(40) Han, L.; Sun, B.; Guo, C.; Peng, G.; Chen, H.; Yang, Z.; Li, N.; Ci, Z.; Jin, Z. Photophysics in Zero-Dimensional Potassium-Doped Cesium Copper Chloride $Cs_3Cu_2Cl_5$ Nanosheets and Its Application for High-Performance Flexible X-Ray Detection. *Adv. Opt. Mater.* **2022**, *10* (6), 2102453.

(41) Ren, Y.; Lü, S. Industrial mass production of novel mixed-halide $Cs_3Cu_2Cl_{5-x}I_x$ and $Cs_5Cu_3Cl_{8-x}I_x$ compounds with greatly enhanced stability and luminescent efficiency by compositional engineering. *Chem. Eng. J.* **2021**, *417*, 129223.

(42) Knutson, J. L.; Martin, J. D.; Mitzi, D. B. Tuning the Band Gap in Hybrid Tin Iodide Perovskite Semiconductors Using Structural Templating. *Inorg. Chem.* **2005**, *44* (13), 4699-4705.

(43) Kawano, N.; Koshimizu, M.; Sun, Y.; Yahaba, N.; Fujimoto, Y.; Yanagida, T.; Asai, K. Effects of Organic Moieties on Luminescence Properties of Organic-Inorganic Layered Perovskite-Type Compounds. *J. Phys. Chem. C* **2014**, *118* (17), 9101-9106.

(44) Smith, M. D.; Jaffe, A.; Dohner, E. R.; Lindenberg, A. M.; Karunadasa, H. I. Structural origins of broadband emission from layered Pb-Br hybrid perovskites. *Chem. Sci.* **2017**, *8* (6), 4497-4504.

(45) Hu, T.; Smith, M. D.; Dohner, E. R.; Sher, M.-J.; Wu, X.; Trinh, M. T.; Fisher, A.; Corbett, J.; Zhu, X. Y.; Karunadasa, H. I.; Lindenberg, A. M. Mechanism for Broadband White-Light Emission from Two-Dimensional (110) Hybrid Perovskites. *J. Phys. Chem. Lett.* **2016**, *7* (12), 2258-2263.

(46) Ma, Z.; Shi, Z.; Qin, C.; Cui, M.; Yang, D.; Wang, X.; Wang, L.; Ji, X.; Chen, X.; Sun, J.; Wu, D.; Zhang, Y.; Li, X. J.; Zhang, L.; Shan, C. Stable Yellow Light-Emitting Devices Based on Ternary Copper Halides with Broadband Emissive Self-Trapped Excitons. *ACS Nano* **2020**, *14* (4), 4475-4486.

(47) Chen, H.; Zhu, L.; Xue, C.; Liu, P. L.; Du, X. R.; Wen, K. C.; Zhang, H.; Xu, L.; Xiang, C. S.; Lin, C.; Qin, M. C.; Zhang, J.; Jiang, T.; Yi, C.; Cheng, L.; Zhang, C. L.; Yang, P. H.; Niu, M. L.; Xu, W. J.; Lai, J. Y.; Cao, Y.; Chang, J.; Tian, H.; Jin, Y. Z.; Lu, X. H.; Jiang, L.; Wang, N. N.; Huang, W.; Wang, J. P. Efficient and bright warm-white electroluminescence from lead-free metal halides. *Nat. Commun.* **2021**, *12* (1), 1421.

(48) Seo, G.; Jung, H.; Creason, T. D.; Yeddu, V.; Bamidele, M.; Echeverria, E.; Lee, J.; McIlroy, D.; Saparov, B.; Kim, D. Y. Lead-Free Halide Light-Emitting Diodes with External Quantum Efficiency Exceeding 7% Using Host–Dopant Strategy. *ACS Energy Lett.* **2021**, *6* (7), 2584-2593.

(49) Zhao, X.; Niu, G.; Zhu, J.; Yang, B.; Yuan, J.-H.; Li, S.; Gao, W.; Hu, Q.; Yin, L.; Xue, K.-H.; Lifshitz, E.; Miao, X.; Tang, J. All-Inorganic Copper Halide as a Stable and Self-Absorption-Free X-ray Scintillator. *J. Phys. Chem. Lett.* **2020**, *11* (5), 1873-1880.

(50) Yang, B.; Yin, L.; Niu, G.; Yuan, J.-H.; Xue, K.-H.; Tan, Z.; Miao, X.-S.; Niu, M.; Du, X.; Song, H.; Lifshitz, E.; Tang, J. Lead-Free Halide Rb_2CuBr_3 as Sensitive X-Ray Scintillator. *Adv. Mater.* **2019**, *31* (44), 1904711.

(51) Gao, W.; Niu, G.; Yin, L.; Yang, B.; Yuan, J.-H.; Zhang, D.; Xue, K.-H.; Miao, X.; Hu, Q.; Du, X.; Tang, J. One-Dimensional All-Inorganic K_2CuBr_3 with Violet Emission as Efficient X-ray Scintillators. *ACS Appl. Electron. Mater.* **2020**, *2* (7), 2242-2249.

(52) Xu, K.-X.; Zhou, Z.; Zhang, J. Phonon-Assisted Upconversion Photoluminescence of a Self-Trapped Exciton in the Rb_2CuCl_3 Single Crystal. *J. Phys. Chem. Lett.* **2022**, 32-37.

(53) Yuan, D. Air-Stable Bulk Halide Single-Crystal Scintillator $Cs_3Cu_2I_5$ by Melt Growth: Intrinsic and Tl Doped with High Light Yield. *ACS Appl. Mater. Interfaces* **2020**, *12* (34), 38333-38340.

(54) Cheng, S.; Beitlerova, A.; Kucerkova, R.; Nikl, M.; Ren, G.; Wu, Y. Zero-Dimensional $Cs_3Cu_2I_5$ Perovskite Single Crystal as Sensitive X-Ray and γ-Ray Scintillator. *Phys. Status Solidi - Rapid Res. Lett.* **2020**, *14* (11), 2000374.

(55) Stand, L.; Rutstrom, D.; Koschan, M.; Du, M.-H.; Melcher, C.; Shirwadkar, U.; Glodo, J.; Van Loef, E.; Shah, K.; Zhuravleva, M. Crystal growth and scintillation properties of pure and Tl-doped $Cs_3Cu_2I_5$. *Nucl. Instrum. Methods Phys. Res.* **2021**, *991*, 164963.

(56) Lian, L.; Zhang, P.; Liang, G.; Wang, S.; Wang, X.; Wang, Y.; Zhang, X.; Gao, J.; Zhang, D.; Gao, L.; Song, H.; Chen, R.; Lan, X.; Liang, W.; Niu, G.; Tang, J.; Zhang, J. Efficient Dual-Band White-Light Emission with High Color Rendering from Zero-Dimensional Organic Copper Iodide. *ACS Appl. Mater. Interfaces* **2021**, *13* (19), 22749-22756.

(57) Rahaman, M. Z.; Ge, S. P.; Lin, C. H.; Cui, Y. M.; Wu, T. One-Dimensional Molecular Metal Halide Materials: Structures, Properties, and Applications. *Small Struct.* **2021**, *2* (4), 2000062.

(58) Li, M. Z.; Xia, Z. G. Recent progress of zero-dimensional luminescent metal halides. *Chem. Soc. Rev.* **2021**, *50* (4), 2626-2662.

(59) Qiu, Y. X.; Ma, Z. M.; Li, Z. W.; Sun, H. Y.; Dai, G. K.; Fu, X. H.; Jiang, H.; Ma, Z. Y. Solely 3-Coordinated Organic-Inorganic Hybrid Copper(I) Halide: Hexagonal Channel Structure, Turn-On Response to Mechanical Force, Moisture, and Amine. *Inorg. Chem.* **2022**, *61* (21), 8320-8327.

(60) Lian, L. Y.; Wang, X.; Zhang, P.; Zhu, J. S.; Zhang, X. W.; Gao, J. B.; Wang, S.; Liang, G. J.; Zhang, D. L.; Gao, L.; Song, H. S.; Chen, R.; Lan, X. Z.; Liang, W. X.; Niu, G. D.; Tang, J.; Zhang, J. B. Highly Luminescent Zero-Dimensional Organic Copper Halides for X-ray Scintillation. *J. Phys. Chem. Lett.* **2021**, *12* (29), 6919-6926.

(61) Song, Z. X.; Yu, B. Y.; Meng, L. Q.; Liu, G. K.; Dang, Y. Y. Air-grown hybrid copper(i) halide single crystals: structural transformations and ultraviolet-pumped photoluminescence applications. *Mater. Adv* **2022**, *3* (5), 2447-2455.

(62) Ma, D.; Lan, Y.; Zhang, D.; Qin, X.; Yang, Z.; He, H.; Dai, X.; Ye, Z.; Cao, X. A one-dimensional organic-inorganic hybrid copper(I)-halide with broadband emission. *Mater. Today Chem.* **2023**, *29*, 101408.

(63) Popy, D. A.; Creason, T. D.; Zhang, Z.; Singh, D. J.; Saparov, B. Electronic structures and optical properties of $(Ph_4P)MX_2$ (M = Cu, Ag; X = Cl, Br). *J. Solid State Chem.* **2022**, *316*, 123626.

(64) Peng, H.; Tian, Y.; Zhang, Z. H.; Wang, X. X.; Huang, T.; Dong, T. T.; Xiao, Y. H.; Wang, J. P.; Zou, B. S. Bulk Assembly of Zero-Dimensional Organic Copper Bromide Hybrid with Bright Self-Trapped Exciton Emission and High Antiwater Stability. *J. Phys. Chem. C* **2021**, *125* (36), 20014-20021.

(65) Fang, S. F.; Zhou, B.; Li, H. X.; Hu, H. L.; Zhong, H. Z.; Li, H. N.; Shi, Y. M. Highly Reversible Moisture-Induced Bright Self-Trapped Exciton Emissions in a Copper-Based Organic-Inorganic Hybrid Metal Halide. *Adv. Opt. Mater.* **2022**, *10* (15), 2200605.

(66) Chen, S. Q.; Gao, J. M.; Chang, J. Y.; Li, Y. Q.; Huangfu, C. X.; Meng, H.; Wang, Y.; Xia, G. J.; Feng, L. Family of Highly Luminescent Pure Ionic Copper(I) Bromide Based Hybrid Materials. *ACS Appl. Mater. Interfaces* **2019**, *11* (19), 17513-17520.

(67) Peng, H.; Wang, X.; Tian, Y.; Zou, B.; Yang, F.; Huang, T.; Peng, C.; Yao, S.; Yu, Z.; Yao, Q.; Rao, G.; Wang, J. Highly Efficient Cool-White Photoluminescence of $(Gua)_3Cu_2I_5$ Single Crystals: Formation and Optical Properties. *ACS Appl. Mater. Interfaces* **2021**, *13* (11), 13443-13451.

(68) Lin, R. C.; Zhu, Q.; Guo, Q. L.; Zhu, Y. M.; Zheng, W.; Huang, F. Dual Self-Trapped Exciton Emission with Ultrahigh Photoluminescence Quantum Yield in $CsCu_2I_3$ and $Cs_3Cu_2I_5$ Perovskite Single Crystals. *J. Phys. Chem. C* **2020**, *124* (37), 20469-20476.

(69) Peng, H.; Yao, S. F.; Guo, Y. C.; Zhi, R. N.; Wang, X. X.; Ge, F. J.; Tian, Y.; Wang, J. P.; Zou, B. S. Highly Efficient Self-Trapped Exciton Emission of a $(MA)_{(4)}Cu_2Br_6$ Single Crystal. *J. Phys. Chem. Lett.* **2020**, *11* (12), 4703-4710.

(70) Liu, X. Y.; Li, Y. Y.; Liang, T. Y.; Liu, W. J.; Fan, J. Y. One-Center and Two-Center Self-Trapped Excitons in Zero-Dimensional Hybrid Copper Halides: Tricolor Luminescence with High Quantum Yields. *J. Phys. Chem. Lett.* **2022**, *13* (5), 1373-1381.

(71) Wang, L.; Sun, H.; Sun, C.; Xu, D.; Tao, J.; Wei, T.; Zhang, Z.-h.; Zhang, Y.; Wang, Z.; Bi, W. Lead-free, stable orange-red-emitting hybrid copper based organic–inorganic compounds. *Dalton Trans.* **2021**, *50* (8), 2766-2773.

(72) Ge, F.; Li, B. H.; Cheng, P. X.; Li, G.; Ren, Z. F.; Xu, J. L.; Bu, X. H. Chiral Hybrid Copper(I) Halides for High Efficiency Second Harmonic Generation with a Broadband Transparency Window. *Angew. Chem.* **2022**, *61* (10), e202115024.

(73) Song, Z.; Yu, B.; Liu, G.; Meng, L.; Dang, Y. Chiral Hybrid Copper(I) Iodide Single Crystals Enable Highly Selective Ultraviolet-Pumped Circularly Polarized Luminescence Applications. *J. Phys. Chem. Lett.* **2022**, *13* (11), 2567-2575.

(74) Mao, P.; Tang, Y. A.; Wang, B. H.; Fan, D. Y.; Wang, Y. Organic-Inorganic Hybrid Cuprous Halide Scintillators for Flexible X-ray Imaging. *ACS Appl. Mater. Interfaces* **2022**, *14* (20), 22295-22301.

(75) Li, M. Z.; Xia, Z. G. Recent progress of zero-dimensional luminescent metal halides. *Chem. Soc. Rev.* **2021**, *50* (4), 2626-2662.

(76) Li, Y. Y.; Zhou, Z. C.; Tewari, N.; Ng, M.; Geng, P.; Chen, D. Z.; Ko, P. K.; Qammar, M.; Guo, L.; Halpert, J. E. Progress in copper metal halides for optoelectronic applications. *Mater. Chem. Front.* **2021**, *5* (13), 4796-4820.

(77) Smith, M. D.; Karunadasa, H. I. White-Light Emission from Layered Halide Perovskites. *Acc. Chem. Res.* **2018**, *51* (3), 619-627.

(78) Smith, M. D.; Connor, B. A.; Karunadasa, H. I. Tuning the Luminescence of Layered Halide Perovskites. *Chem. Rev.* **2019**, *119* (5), 3104-3139.

(79) Li, S.; Luo, J.; Liu, J.; Tang, J. Self-Trapped Excitons in All-Inorganic Halide Perovskites: Fundamentals, Status, and Potential Applications. *J. Phys. Chem. Lett.* **2019**, *10* (8), 1999-2007.

(80) Zhang, Z.; Fattal, H.; Creason, T. D.; Amiri, M.; Roseborough, A.; Gilley, I. W.; Nyman, M.; Saparov, B. Investigation of the Solution Chemistry of Hybrid Organic-Inorganic Indium Halides for New Material Discovery. *Inorg. Chem.* **2022**, *61* (33), 13015-13021.

(81) Zhang, K.; Wang, S.; Yi, L. Defect emission in $Cs_3Cu_2I_5$ and $CsCu_2I_3$ halide films. *J. Lumin.* **2023**, *254*, 119516.

(82) Gong, X.; Voznyy, O.; Jain, A.; Liu, W.; Sabatini, R.; Piontkowski, Z.; Walters, G.; Bappi, G.; Nokhrin, S.; Bushuyev, O.; Yuan, M.; Comin, R.; McCamant, D.; Kelley, S. O.; Sargent, E. H. Electron–phonon interaction in efficient perovskite blue emitters. *Nature Mater* **2018**, *17* (6), 550-556.

TOC Graphic

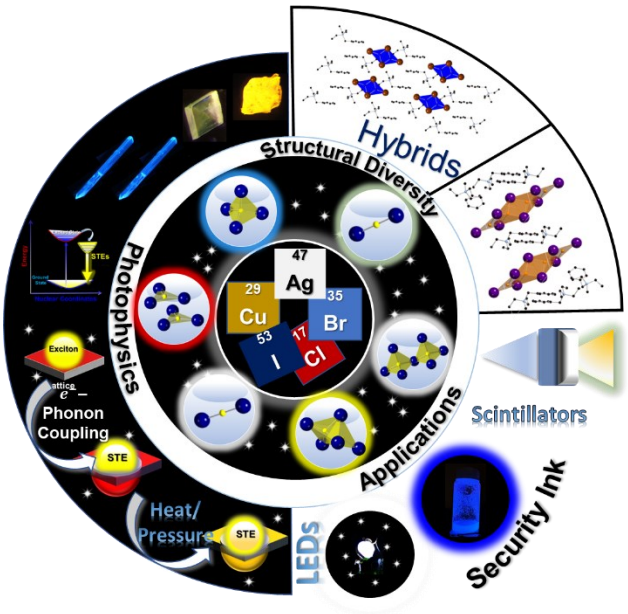
Hybrids
Structural Diversity
Photophysics
Applications
Scintillators
Security Ink
LEDs
Heat/
Pressure
STE
Exciton
Phonon
Coupling
47
Ag
29
Cu
35
Br
53
I
17
Cl